

UNIVERSITY OF EXETER

Modelling the Effects of a Human on the Immediate Environment using CFD Combined with a Human Comfort Model

Individual Report I-2

French, Tom

April 2013

Candidate Number: 006105

Student Number: 590018127

Supervisor: Dr Gavin Tabor

Abstract

This report outlines the project carried out regarding the effect of humans on the immediate environment. Work was carried out with the end goal to create a CFD model coupled with the IESD Fiala human thermal comfort model. This was achieved on a manual scale for a natural ventilation setup as well as in partnership with Locci for the model of Harrison Room 170. The final coupled model simulated how Room 170 responded to human presence, and also how the human responds to its local environment. Using both of these models, a successful simulation showed that a single human will increase the immediate environmental temperature of Room 170 by 0.26 degrees, and by roughly 1.72 degrees in the naturally ventilated case. The data recorded was compared against theory and previous work which displayed the same temperature trends. This report covers a study of previous works and theoretical understanding, before looking at the methodology involved, the results achieved and the importance and effect of these results on future work.

Keywords

Computational Fluid Dynamics, Human Comfort, Fiala Model, Heat Transfer, Human Geometry, Natural Ventilation

Acknowledgements

I would like to thank Dr Gavin Tabor for his mentorship and productive input throughout the project. I would also like to extend my gratitude to Edward Shorthouse and Dr Matt Eames for their expertise in the project topic and offering assistance throughout the project. My thanks are also extended to each of the group members for working efficiently as a team in order to make the aims of this project achievable; Patrick Tompsett, Alex Smith, Jamie Bunting, Gianluca Locci, Katrina Pammatmat and Matthew Dalladay-Simpson.

Contents

Abstract.....	i
Keywords.....	i
Acknowledgements	i
Table of Figures.....	iv
Table of Tables	v
1. Introduction	1
2. Aims and Objectives.....	2
3. Review of Previous Works	3
3.1. Human Thermal Comfort Modelling.....	3
3.2. Simulating Human Heat Transfer with CFD	5
4. Theoretical Understanding	9
4.1. The Navier-Stokes Equations	9
4.2. Turbulence Modelling.....	9
4.2.1. K-epsilon Models	9
4.2.2. K-omega Models	10
4.3. Heat Transfer Equations	10
4.4. Buoyance Driven Flow	11
4.4.1. Implementation in Fluent	11
4.5. IESD Fiala Model	12
4.6. Laser Scanning.....	13
4.7. Thermal imaging.....	13
5. Methodology and Design	14
5.1. Initial Design Work	14
5.1.1. Solidworks Design.....	14
5.1.2. David Laserscanner	15
5.2. Preliminary Heat Transfer Simulations	16
5.3. Using the IESD-Fiala Model	17
5.4. Split Human	20
5.5. Free Convection Human Geometry	21
5.6. Mesh Convergence Study	25
5.7. Free Convection Coupling	26
Step 1	27

Step 2	27
Step 3	28
Step 4	28
5.8. Coupling within Room 170 Model; Working with Gianluca Locci	28
6. Results	29
6.1. Free Convection Coupling	29
6.2. Human and Room 170 Integration.....	32
7. Discussion and Comparison of Results	34
8. Sustainability	36
8.1. Society	36
8.2. Environmental.....	36
8.3. Economy	36
9. Project Management.....	37
9.1. Group Work	37
9.2. Budgeting.....	37
9.3. Health and Safety.....	37
10. Conclusion.....	38
11. Future Work.....	39
References	I
Appendix A	IV
Appendix B.....	V
Appendix C.....	VI
Appendix D	IX
Appendix E.....	XII

Table of Figures

Figure 1 – Geometry Used by Murukami et al. [13]	5
Figure 2 – Clothed Human Geometry Divided into 59 Surfaces [2].....	6
Figure 3 – High Quality Surface Meshing used by Cropper et al. [2].....	7
Figure 4 – Laser Scanning Rig for Thermal Manikin Geometry [19].....	8
Figure 5 – Schematic of the Mathematical Process Involved in the IESD Fiala Model [29] ..	12
Figure 6 – Example Thermal Image of Group Member.....	13
Figure 7 – Simple Human Geometry Generated on Solidworks	14
Figure 8 – David Laser Scanning Process Including Calibration, Scanning, Aligning Scans and Fusion	15
Figure 9 – Basic Cylinder Setup.....	16
Figure 10 – Temperature Contours across Midplane (K).....	16
Figure 11 – Example BC File	17
Figure 12 – Example Configuration File	17
Figure 13 – Executional File Run to simulate 1000 minutes	18
Figure 14 – Solidworks Human Geometry Split into Faces compared with Split Model by Cropper et al. [14].....	20
Figure 15 – Detailed Mesh with Surface Sizing	21
Figure 16 – Temperature Contours of Male in Briefs	22
Figure 17 – Velocity Vectors of Male in Briefs	22
Figure 18 – Temperature Contours of Male in Full Clothing	23
Figure 19 – Setup of Volume with Vents	24
Figure 20 – Data Values from Midplane to Display Mesh Convergence	26
Figure 21 – Example Temperature Convergence from Fiala Output Files	27
Figure 22 – Room Temperature Convergence	29
Figure 23 – Temperature Contours from XY and YZ Midplanes	30
Figure 24 – Velocity Vectors in Y Direction in Natural Convection Domain	30
Figure 25 – Position of Sample Lines within the Domain	31
Figure 26 – Temperature Variance above the Head (Left) and Behind the Body (Right)	31
Figure 27 – Temperature Convergence in Room 170	32
Figure 28 – Temperature Contours Before and After the Impact of the Human.....	33
Figure 29 – Convection Coefficients for Both Cases Compared with Work by Cropper et al.	34
Figure 30 – Management Gantt chart	IV
Figure 31 – Mesh Refinement at Human Surface with Extra Detail at Boundary Layer.....	V
Figure 32 – Contours on Human Surfaces showing Fiala Output Temperatures.....	VII
Figure 33 – Volume Rendering of Temperature for Free Convection Case	VIII
Figure 34 – Volume Rendering of Velocity for Free Convection Case	VIII
Figure 35 – Technical Drawing of Room 170 [32]	IX
Figure 36 – Setup of Human Geometry in Room 170 [32]	IX
Figure 37 – Initial Mesh used by Locci	X
Figure 38 – Mesh of Room 170 Containing the Human Geometry	X
Figure 39 – Room 170 Setup Details.....	XI
Figure 40 – Method Used for Obtaining Ambient Conditions for Fiala Input.....	XI

Figure 41 – Thermal Images of Tompsett (top) in t-shirt and trousers, and French (bottom) in jumper and trousers XII

Table of Tables

Table 1 – Timeline of Well-known Human Comfort Models	4
Table 2 – Faces the Human is Split into by the Fiala Model and their Respective Areas [37]	19
Table 3 – Details of the Mesh Convergence Study	25
Table 4 – Details of Mesh Convergence Study	V
Table 5 – Fiala Outputs for Coupling with Room 170.....	VI
Table 6 – Inputs and Outputs for Fiala Free Convection Coupling.....	VI

1. Introduction

Over the last fifteen to twenty years it has become more and more apparent that global temperatures have been increasing [1]. This can be put down to one main reason; the changing nature of human activity. Whilst effort is being made to reduce emissions which lead to increased temperatures, such as utilising wind turbines and solar panels, it is also important to provide solutions which ameliorate the effects of the changing conditions. One such problem posed by the rising temperatures is the effect on the built environment. Extreme conditions will unquestionably have an impact of inhabitants in urban areas, meaning that building design could play a key role in dealing with these conditions. It is therefore important to understand how a room or a building responds to changing weather conditions; not only how the internal environment changes, but how inhabitants adjust, and in turn the effect that the inhabitants have on the immediate environment.

Another issue related to global warming is the diminishing global resources. In order to conserve these resources, natural ventilation systems are becoming more and more popular in modern buildings. These systems are used as opposed to HVAC (heating, ventilation and air conditioning) systems. CFD (Computational Fluid Dynamics) is now often used to predict the performance of building designs as natural ventilation can be a relatively simple problem to set up [2].

However, whilst CFD is often used to simulate the inside of buildings, most previous works do not consider the contribution of humans to heat generation. Whilst the heat generation from humans can be small, there is still a noticeable change to the environment, especially if there is a large number. This group project as a whole aims to model a detailed built environment containing a number of heat sources as well as humans. Looking in further detail, the results achieved will be compared with experimental data recorded over the course of the project. In order to achieve this goal, the group was initially split into three subgroups; human, room environment and electronics.

As a member of the human group, the work in this report focuses on the heat generation from a human body, combining the IESD-Fiala human comfort model (discussed in previous work and theoretical understanding) and CFD in ANSYS Fluent. It first looks at creating human geometries before simulating heat transfer in Fluent. It then goes on to incorporate the human comfort model and a simplistic coupling of the two. The latter stages of the report look at working together with the room group to model the human geometry inside Room 170 as accurately as possible, with various other heat sources and velocity inlets also taken into account. These results are then compared with results from previous works and theory.

The report will be structured to first cover previous works and theoretical background, before outlining the methodology used to carry out the objectives. It will go on to display detailed results and analysis as well as details about the management of the project including a work plan.

2. Aims and Objectives

As a group, the aim was to generate a working computational model of Room 170 in the Harrison building and compare temperature and humidity values with experimental data recorded. However, as an individual a number of direct objectives were defined.

As stated in the G1, the following deliverables were defined at the start of the project:

- Develop a set of human geometries ranging from basic to complex using Solidworks.
- Scan a human body using David Laserscanner software, along with using an infra-red camera to gain thermal heat loss information.
- Create a simple heat transfer simulation in ANSYS Workbench.

Due to constraints and changes made during the course of the project, these objectives were modified in order to spread the work in the subgroup evenly between Patrick Tompsett and myself.

The following modified objectives were defined for this individual part of the project:

- Develop a moderately accurate human geometry in Solidworks with which to carry out simulations.
 - In reality, a highly detailed human model was unnecessary, as computing power would restrict precision, whilst the meshing quality would suffer.
- Attempt to scan a small manikin using the David Laserscanner software.
 - A full scale human would be challenging due to the equipment available on the project budget. Keeping a human in an exact position for multiple scans would also be difficult in order to produce an accurate geometry.
- Produce thermal images using an infra-red camera to gain heat loss information.
- Create a simple heat transfer simulation in ANSYS Workbench.
- Run a basic calculation using the IESD-Fiala human comfort model.
- Create a CFD model coupled with the Fiala model in a control volume.
- Integrate the human CFD/Fiala model with the room model of Gianluca Locci.

It was decided that the IESD-Fiala model would become part of this individual work as a large amount of reading had been carried out into the subject. This tailored the project to look at the response of humans to different environments/activity levels and apply this to the CFD in the chosen built environment.

3. Review of Previous Works

3.1. Human Thermal Comfort Modelling

As a human is placed in an environment, a number of factors affect how the human's comfort responds. Naturally a very hot environment will cause the human to sweat in order to cool down the body, whilst a cold environment will cause the body to shiver to retain heat. As the human body is a highly complex system which includes multiple organs, muscles, tissue groups, blood and bones, predicting its response is a complicated process. Whilst this is clearly very difficult, researchers have been attempting to generate models in which the comfort of a human can be predicted based on external factors. Thermal comfort can be hard to define, but was designated (American Society of Heating, Refrigerating, and Air-Conditioning Engineers, 1966) in 1966 as "that state of mind which expresses satisfaction with the thermal environment" [3]. In order to obtain information with which to produce a predictive model, researchers have for years been running experiments that subject humans to varying conditions; very hot to very cold, varying humidity, air velocity and activity levels.

Since the early 1970s, there have been a number of models that range in complexity. According to Fu et al., the different models can be classified as one of three categories: one node thermal models, two-node thermal models and multi-node thermal models [4]. One node models represent the human as only one node and predict responses based on formulae obtained from experiments. Two node models on the other hand are lumped parameter models that divide the body into two concentric shells, where the inner shell represents the internal organs, bone, muscle and subcutaneous tissue, and the outer shells represents the skin layer. Multi node models expand on the two node model, containing more shells with each layer containing the energy balance equation separately [4] [5]. Two of the earliest models that were widely used are the Fanger (1982) and the Gagge two-node model (1986) [3]. Both of these models work by solving heat balance equations for the human body. The heat and mass exchange with the environment is modelled using a one-dimensional approximation, making both models relatively simple. The Fanger model does not attempt to simulate transient or thermal regulation, making it even simpler. Whilst these two models are both available to use, the lack of user friendly interfaces seemed to put off many potential users [6]. More complex systems were created during the earlier years, including the Wissler model which divides the body into hundreds of segment. The complexity at the time made it difficult to use effectively. Advances in technology and computational power have allowed further developments and more complicated models. The Smith-FU model for example uses a three thousand node finite element model to simulate the body [4].

The earliest models focus mainly on the thermal physiology of the human body, somewhat neglecting simulating the heat and mass transport through clothing. Due to high levels of complexity; air gaps between clothes and skin, constant change in position of clothing and thermal properties, clothing was generally ignored. In some cases it was added but only as an extra layer of insulation that could be easily modelled [7]. Some of the most notable comfort models are displayed in Table 1.

Table 1 – Timeline of Well-known Human Comfort Models

Date	Author	Description
1964	Wissler	225-node finite element model
1970	Fanger	PMV steady state model
1970	Stolwijk	25-node basic heat flow model
1986	Gagge et al.	2-node basic heat flow model
1990	De Dear and Ring	40-layer finite difference skin model
1992	Jones and Ogawa	2-node with transient response
2002	Tanabe	Modified Stolwijk model
1999-2003	Fiala et al	Multi-node Heat flow model

Despite the complexity difference amongst the models, all of them share similar features. Each model attempts to somehow evaluate the heat and moisture exchange with the environment. It must also determine either the steady state or the transient balance between heat generated in the body (metabolism) and heat dissipated to the environment (respiration, evapotranspiration, convection, radiation and/or conduction).

Some of the newer models, such as the Tranmod model by Jones and Ogawa, focus on detailed transient models of heat and moisture transport through clothing, but use relatively simple thermal models of the body [8]. The most recent models are the Tanabe and IESD-Fiala models, which go into much more detail predicting both the overall and local physiological responses. This means the interior of the body is simulated, as well as how the exterior of the body reacts, in terms of moisture and heat loss from the body. Tanabe et al. developed a model that was based on the early work of Stolwijk. The 65-node thermoregulation model consisted of 16 body segments that corresponded to a thermal manikin. By carrying out a large number of experiments on the thermal manikin, convective and radiant heat transfer coefficients were derived. This allowed a numerical model to be developed for both standing and sitting postures [9]. The model incorporates data of an average man with a weight of 74.43kg and a surface area of 1.87m², and was shown to provide sufficient accuracy when compared with experimental results [10].

The model considered the most advanced and accurate is the work developed by Dr Dusan Fiala between 1998 and 2003. The model itself was derived using thermal sensation votes from over 200 male and female subjects, written in PASCAL as a computer program and is available in the public domain with permission [11]. In order to model both the interior and exterior heat transfers, the program was developed in two stages to incorporate both interacting thermoregulation systems: the controlling active system, and the controlled passive system.

Developed in 1991, the active model simulates thermoregulatory responses. This includes suppression (vasoconstriction) and elevation (vasodilatation) of blood flow, sweat excretion and shivering. It was developed by measuring responses to a range of temperatures (5-50°C) and exercise levels (0.8-10 MET (metabolic equivalent of task where 1 MET = 4.18kJ/kg.h)) [12]. It is known as the controlling active system as it looks at the exterior environment, which will in turn control how the interior of the body responds in the passive system.

Developed after the active system, the passive system (1993) uses a multi segmental multi-layered representation of a human body. The body contains subdivisions which include anatomic, thermo physical and thermo physiological properties. It accounts for all heat transfer inside the body; blood circulation and metabolism, and at the surface such as convection, evaporation and radiation. The IESD Fiala model has been widely subjected to extensive validation and verification tests, as many before had not. As it is regarded as the most up to date and accurate model available, it will be used further in this project. More detail about the theory behind the model can be found in section 4.5.

3.2. Simulating Human Heat Transfer with CFD

CFD has been improving greatly over recent decades, with the increase in computing power and memory directly proportional to its rise. With the programs now available, simulations can be run with meshes containing millions of cells, allowing more and more precise simulations to be run. With the modern reliability of CFD, providing the case is set up correctly, it has become a very popular method of measuring flow, often preferred to experimental data using sensors.

Without a highly complicated setup, it is difficult to model the inside of a human using CFD. Therefore it is often ignored, and the skin temperatures or heat transfer coefficients are used in order to model the external environment. This means that the effect on the built environment can be displayed. However without knowing the inner workings of the human, predicting its effect on the environment is more challenging. In an attempt to cover both sides of the simulation, researchers have made numerous attempts to incorporate thermal comfort models into CFD calculations. This in theory would provide an accurate model of how the local environment affects the body and vice versa.

One of the first attempts at full integration came from S. Murukami et al. in 2000. Using a vase-shaped smooth figure (displayed in Figure 1) to represent a human, the CFD heat model was coupled with Gagge's 2-node thermal regulatory model. The CFD was used to simulate the flow field for given temperature boundary conditions. The 2-node model was then used to provide predicted skin temperature distributions corresponding to the local sensible heat loss

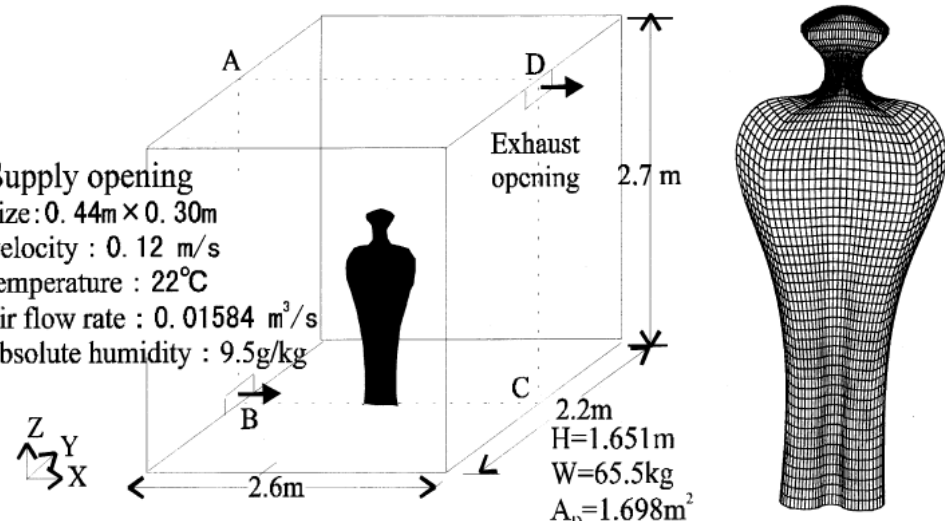


Figure 1 – Geometry Used by Murukami et al. [13]

values calculated by the CFD. The geometry used smoothed the legs and arms into one body in order to generate a high quality mesh. The CFD used the k-epsilon turbulence model for a low Reynolds number (due to low air velocity). Gebhart's adsorption factor method was used for thermal radiation and the Monte Carlo method was used for CFD view factors. It was shown that the predicted results were very close to those of a human body in a similar situation [13].

Another attempt at coupling came when Tanabe et al. (2002) reported the integration of the 65MN model with CFD and radiation code. Using a 3D model of an unclothed male, steady-state results were shown to include the effect of solar (short wave) radiation. Convection from the body, however, was calculated using heat transfer coefficients rather than the CFD simulation [10]. Another effort came from Omori et al. (2004) who carried out a process coupling CFD code with Fanger's model.

Perhaps the most recent and successful study by Cropper et al. used the IESD Fiala model in conjunction with CFX CFD code to predict the response of the body to the local environment. A 3D geometry was designed in order to comply with the Fiala model. This was done by generating two fixed body shapes; a nude figure made up of 56,000 surface cells and a surface area of 1.82m^2 , and a clothed figure made up of 65,000 cells and a surface area of 2.15m^2 . The Fiala model outputs results files for 59 body faces so the 3D geometries were divided into the corresponding parts. This can be seen in Figure 2 below. In order to simplify the solution

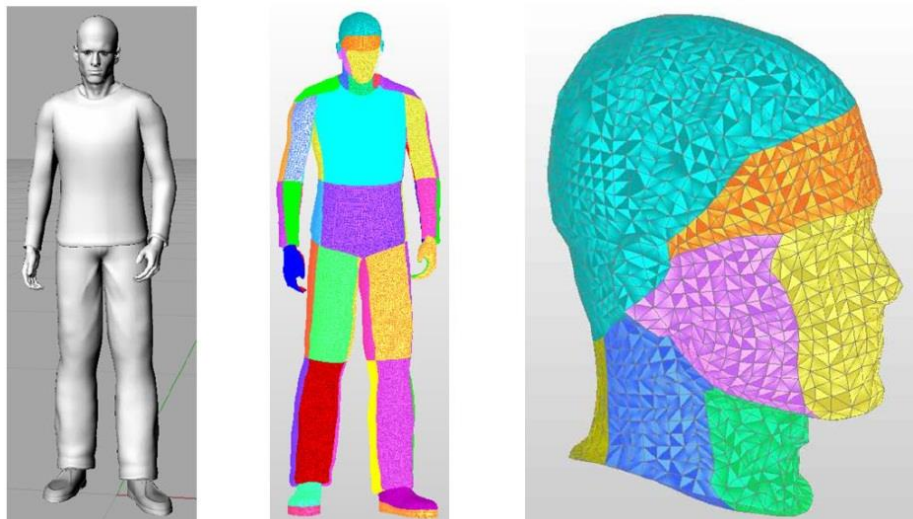


Figure 2 – Clothed Human Geometry Divided into 59 Surfaces [2]

slightly, detailed zones such as the ears and fingers were smoothed over in the mesh. This saved computational power for a very fine mesh that would ultimately make only a small difference. The IESD-Fiala model in its stand-alone state, predicts the body's response to local conditions that change over time. This research used the model in a steady state fashion, meaning it was run as if the body was exposed to the same conditions for a long time. This meant that the model achieved convergence each time it was run. Air flow and heat transfer were modelled in CFX, with the human the only heat source in the domain. All other surfaces were modelled as adiabatic. The use of CFX allowed for further code to be entered which was used in the coupling process. This meant that body surface temperatures and moisture levels

could be changed during the simulation. With the CFD set up using a transient implicit solver of the evolution of flow from the initial conditions, the Fiala model outputs were entered as inputs periodically throughout the solution cycle. Unlike the work by Murukami et al., Cropper et al. carried out the coupling during only one CFD simulation, a more time efficient method [14].

The process was successfully implemented by setting the model up to consist of a clothed male standing in a naturally ventilated space. Predetermined boundary conditions for temperature and humidity, along with the Fiala model inputs allowed for a successful buoyancy driven natural ventilation flow driven by the skin temperatures. The method was also considered efficient as the data exchanges used minimal extra computing resources [2].

It has been demonstrated by a number of researchers that simulating heat transfer from a human in CFD can be significantly aided by incorporating a human thermal comfort model. Whilst validation of these models is uncertain (bar the Fiala model) they can offer a degree of accuracy that cannot be offered by other methods. Therefore, it has been used successfully and considered a useful tool. The work carried out in this project will be done in ANSYS Workbench using Fluent's code. The coupling process by Cropper et al. was done using CFX which allows code to be entered. For this reason a computational coupling process is slightly beyond the scope of this project. One key challenge working with CFD is generating a high quality mesh for running the calculations. A poor quality mesh can result in the residuals not converging and therefore incorrect results. In order to measure the flow around the human, it is vital that the mesh is designed to be as precise as possible in the important areas, i.e. at the surfaces of the human. This can be done using a surface meshing tool. Setting a cell size at a surface allows the mesher to extrude up from the surface and create small cells alongside it. This is much more reliable than meshes that contain cells in which only their corners touch the surface. The mesh used by Cropper et al. can be seen in Figure 3 below, with more dense areas around the human and walls where boundary layer flow is likely to be significant.

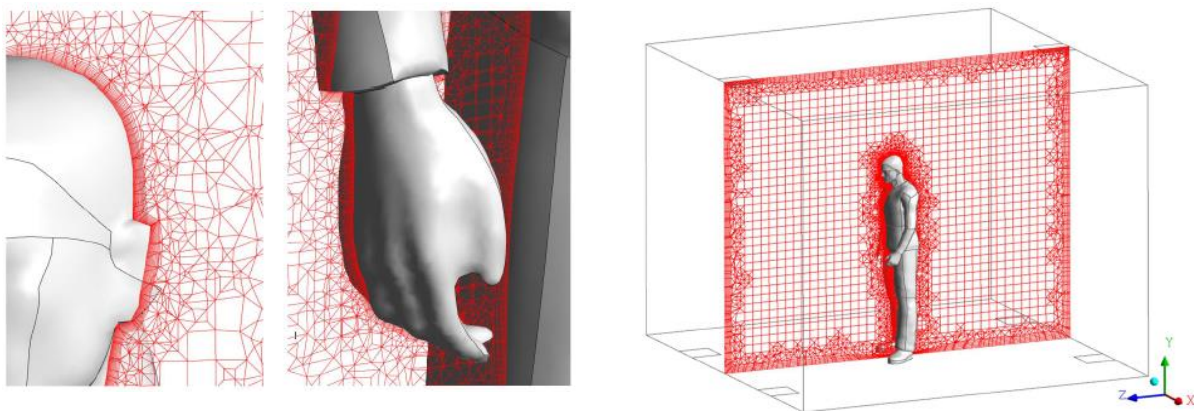


Figure 3 – High Quality Surface Meshing used by Cropper et al. [2]

Another challenge when modelling the heat flow around the human is the buoyancy driven flow and how to model it. This will be discussed further in the theory, along with the Boussinesq approximation. This project will look at a coupling process similar to that of

Cropper but at a slightly more basic level. The coupling process will also be transferred across into the built environment Room 170 for the group project.

Another aspect of this project that must be looked at is the modelling of naturally ventilated rooms. Whilst this area was looked at mainly by the room group, having an understanding is important. Work carried out by Hajdukiewicz simulated airflow around a simple room containing a human. Wireless egg-whisk sensors were also set up and air velocities and temperature values were taken for comparison purposes. The boundary conditions were taken from these sensors and local weather conditions. The room also contained lamps, radiators and computer as heat sources. The sixteen sensors correlated well with the CFD for temperature readings, although the recorded values of air velocity were not accurately predicted by the CFD model. Potential improvements could be made by adjusting high importance parameters such as the outside air temperature, air velocity Z component and human heat flux [15]. Loomans et al. looked at a number of humans sitting in a room, modelled as a series of cylinders and cuboids. This was a relatively old study and was therefore limited by computational power. Despite this, air velocities and temperatures were successfully predicted in the ventilated room [16]. This research has been looked into further by Smith in this project [17], with a similar CFD problem set up as a validation project.

A study by Gao et al. [18] reviewed works into heat transfer around a human. One such study by Davidson et al. used a geometry generated from a laser scan. A thermal manikin was scanned using a set up rig in a laser scanning workshop (Figure 4) [19].

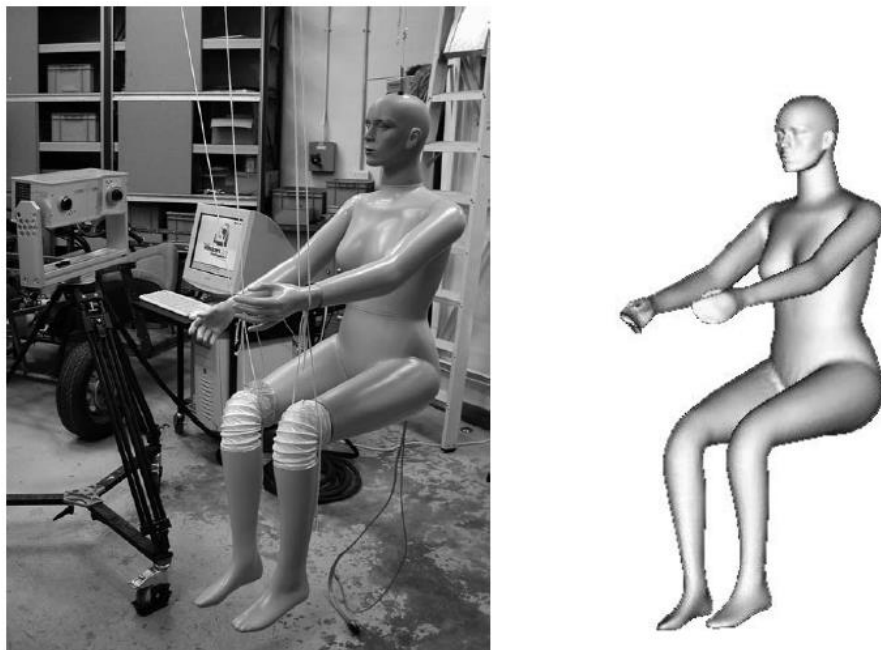


Figure 4 – Laser Scanning Rig for Thermal Manikin Geometry [19]

This allowed for experimental values to be directly compared to the CFD predicted results as the geometry is exactly the same. As previously mentioned in the I1 report [20], this project will attempt to use laser scanning technology as well. However due to financial restraints, high quality results were always unlikely.

4. Theoretical Understanding

4.1. The Navier-Stokes Equations

CFD is governed by a set of equations called the Navier Stokes Equations, which refer to the incompressible form of the momentum equation. These equations also comprise expressions for conservation of mass and energy for general motions [21] [22]:

$$\frac{D}{Dt}(\rho) = 0 \quad \text{Equation 1}$$

$$\frac{D}{Dt}(\rho U_i) = -\frac{\partial p}{\partial x_i} + \frac{\partial}{\partial x_j} \left(\frac{\mu \partial U_i}{\partial x_j} - \rho u_i u_j \right) - \rho \beta g_1 (\theta - \theta_{ref}) \quad \text{Equation 2}$$

$$\frac{D}{Dt}(\rho \theta) = \frac{\partial}{\partial x_j} \left(\frac{\mu}{Pr} \frac{\partial \theta}{\partial x_j} - \rho \theta u_j \right) \quad \text{Equation 3}$$

In which $u_i u_j$ are the Reynolds stresses and θu_j are the turbulent heat fluxes which should be modelled.

4.2. Turbulence Modelling

All CFD simulations that model flows over a certain Reynolds number require a turbulence model. Due to the slightly unpredictable nature of turbulent flow, a number of models have been developed which attempt to model the flow accurately. Whilst it is difficult to find one specific model that is correct, some models are more appropriate for particular types of flow. This project focuses mainly on flow generated by heat i.e. buoyancy driven flow. Flow velocities are expected to be low whilst it will be important to be precise close to the human (modelled as a wall). The work also looks briefly at driven flow, with an inlet velocity incorporated.

4.2.1. K-epsilon Models

One of the most common turbulence models, the K-epsilon model consists of two equations, meaning it includes two extra transport equations to represent the turbulent properties of the flow. This allows the model to account for history effects like convection and diffusion of turbulent energy. The first transported variable is turbulent kinetic energy k , which determines the energy in the turbulence, while the second transported variable, turbulent dissipation ϵ , determines the scale of the turbulence. The $k-\epsilon$ model is considered industry standard. Generally speaking it is considered to offer a good compromise in terms of accuracy and robustness. Whilst the standard $k-\epsilon$ model within Fluent uses the scalable wall-function approach to improve robustness and accuracy when the near-wall mesh is very fine, it has been shown to be less suitable for boundary layer separation [23].

4.2.2. K-omega Models

The standard k- ω model solves for k and ω , the specific dissipation rate (ϵ/k) based on Wilcox [24]. It shows superior performance for wall bounded and low-Re flows. It can also account for transitional flow, free shear and compressible flows, although this will not be required. A variant of the k- ω model is the SST k- ω model. This combines the original Wilcox model for use near walls and the standard k- ϵ model away from walls for a blending function [25]. This makes it a suitable model for this project as the simulations involve free stream and buoyancy along with boundary layer flow with natural convection near walls.

The SST (Shear Stress Transport) k- ω model was chosen for simulations in this work due to the reasons above. It was also used by Cropper et al. for a similar application. The governing transport equations are displayed below:

$$\frac{\partial}{\partial t}(\rho k) + \frac{\partial}{\partial x_i}(\rho k u_i) = \frac{\partial}{\partial x_j} \left(T_k \frac{\partial k}{\partial x_j} \right) + G_k - Y_k + S_k \quad \text{Equation 4}$$

$$\frac{\partial}{\partial t}(\rho \omega) + \frac{\partial}{\partial x_i}(\rho \omega u_i) = \frac{\partial}{\partial x_j} \left(T_\omega \frac{\partial \omega}{\partial x_j} \right) + G_\omega - Y_\omega + D_\omega + S_\omega \quad \text{Equation 5}$$

In these equations G_k is the generation of turbulent kinetic energy, G_ω is the generation of ω , T_k and T_ω are the effective diffusivity of k and ω , Y_k and Y_ω are the dissipation of k and ω due to turbulence, D_ω is the cross-diffusion term and S_k and S_ω are user-defined source terms. All of these terms are calculated using further equations that can be found in the ANSYS Fluent theory guide [26].

4.3. Heat Transfer Equations

Heat transfer occurs in three different ways: conduction, convection and radiation. It is unlikely that conduction will have a large effect on the experiment, apart from perhaps transferring heat to the floor from the body, but this will be minimal. Due to the relatively low temperatures of the human surface, radiation is also likely to have a very small effect, making natural and forced convection the key transfer modes by which the human body heats the surroundings.

Convection is the transfer of thermal energy from one place to another by the movement of fluid or gases. Generally speaking it is the dominant form of heat transfer in fluids. Free convection is when fluid motion is caused by buoyancy forces that result from the density differences due to variation of temperature in the fluid. When the fluid is in contact with a hot surface, its molecules separate and scatter, causing the fluid to be less dense and rise.

Convective heat loss is described by Newton's law of cooling:

$$\frac{dQ}{dt} = h \cdot A(T_{env} - T(t)) = -h \cdot A \Delta T(t) \quad \text{Equation 6}$$

Where Q = thermal energy in Joules, h = heat transfer coefficient ($\text{W}/\text{m}^2\text{K}$), A = surface area of the body (m^2), T = temperature of surface (K) and T_{env} = temperature of the environment (K).

4.4. Buoyance Driven Flow

The Boussinesq Approximation is used in buoyancy driven flow. It states that density differences are sufficiently small to be neglected, except when they are multiplied by g , the acceleration due to gravity. The essence of the approximation is that the difference in inertia is negligible but gravity is sufficiently strong to make the specific weight appreciably different between the two fluids. The advantage of the approximation is that a flow made up of two fluids of density ρ_1 and ρ_2 needs only consider one single density ρ because the difference $\Delta\rho = \rho_1 - \rho_2$ is negligible. The use of dimensionless analysis shows that under these circumstances the only sensible way that acceleration due to gravity g should enter into the equations of motion is in the reduced gravity g' :

$$g' = g \frac{\rho_1 - \rho_2}{\rho}$$

Equation 7

The problem is therefore simpler because the ratio ρ_1/ρ_2 does not affect the flow as the Boussinesq approximation states that it may be assumed to be one [27].

4.4.1. Implementation in Fluent

Modelling natural convection with the Boussinesq model in Fluent allows for faster convergence than by setting up the problem with fluid density as a function of temperature. The model treats density as a constant value in all solved equations, except for the buoyancy term in the momentum equation: [28]

$$(\rho - \rho_0)g \approx -\rho\beta(T - T_0)g$$

Equation 8

In this equation ρ_0 is the constant density of the flow, T_0 is the operating temperature, and β is the thermal expansion coefficient. This equation is obtained by using the Boussinesq approximation:

$$\rho = \rho_0(1 - \beta\Delta T)$$

Equation 9

This eliminates ρ from the buoyancy term. As long as density changes are small, as they are in this work, the approximation is valid. Specifically, it is valid when:

$$\beta(T - T_0) \ll 1$$

Equation 10

Theory for solution methods was unavailable, however 2nd order spatial pressure discretisation was utilised on the recommendation of the Fluent User Guide [28].

4.5. IESD Fiala Model

The theory behind the Fiala model is very complicated as it involves heat transfer through various different body parts and tissues with respect to time. The Fiala model divides the body into 12 spherical and cylindrical body components: head, face, neck, shoulders, thorax, abdomen, upper and lower arms, hands, upper and lower legs, and feet. All of these cells are built of concentric tissue layers: brain, lungs, bones, muscles, viscera, fat and skin.

The foundation equation is for bio heat transfer. This models the bio-heat transfer for polar and spherical coordinates. The equation is displayed below:

$$\rho c \frac{\partial T}{\partial t} = k \left(\frac{\partial^2 T}{\partial r^2} + \frac{\omega}{r} \frac{\partial T}{\partial r} \right) + \rho_{bl} w_{bl} C_{bl} (T_{bla} - T) + q_m \quad \text{Equation 11}$$

In this equation ρ (kg/m^3) is tissue density, c (J/kg/K) tissue heat capacitance, T ($^\circ\text{C}$) tissue temperature, t (s) time, k (W/m/K) tissue conductivity, r (m) radius, ω is a geometry factor ($\omega = 1$ for polar co-ordinates, $\omega = 2$ for spheres), T_{bla} ($^\circ\text{C}$) arterial blood temperature, ρ_{bl} (kg m^{-3}) density of blood, w_{bl} ($\text{m}^3 \text{s}^{-1} \text{m}^{-3}$) blood perfusion rate, C_{bl} ($\text{J kg}^{-1} \text{K}^{-1}$) heat capacitance of blood, and q_m (W m^{-3}) metabolism [29].

This forms the basis for many other complicated equations and notations used by the Fiala model, such as for blood circulation, shivering and changes in local metabolism. Of course these all change with respect to time and to each other, hence why it is all run computationally. Figure 5 shows a schematic of the processes involved in calculating the human comfort.

All of the relevant theory can be found in literature written by Dr Fiala, as well as in the IESD Fiala model software which is free to download with permission [29] [12].

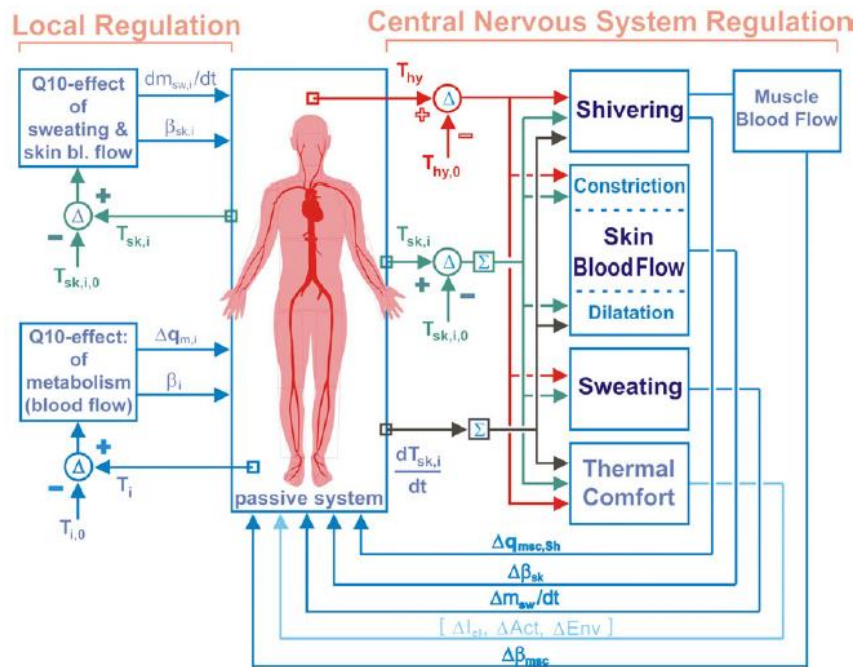


Figure 5 – Schematic of the Mathematical Process Involved in the IESD Fiala Model [29]

4.6. Laser Scanning

A small part of this project looked at generating a human geometry not only from CAD, but also by using laser scanning software. The method attempted was the free David Laserscanner software. Requiring only a small line laser and an autofocus webcam, the set up was relatively simple.

Three-dimensional (3D) laser scanning based 3D shape modelling is a non-contact active measuring technique for developing a digital representation of the 3D shape of a real object. A 3D laser scanner can quickly scan the subject surface many times to obtain sets of 3D coordinates of spatial geometric sampling points (called point clouds), which can then be used to reconstruct the shape of the subject [30]. The David laser scanner uses a hand-held line laser scanner and a camera. For laser scanning to work, the laser ray has to intersect two things at once: the surface and the reference geometry (in this case the 90° background boards) [31]. The visible intersection is used to calibrate the laser. With this knowledge, we can triangulate new 3D point coordinates of the body's surface by intersecting the laser plane with the projecting rays. The signals received from the laser to the camera are stored and the coordinates generate a 3D model.

4.7. Thermal imaging

A thermo graphic or infrared camera is a device that forms an image using infrared radiation. As all objects emit a certain amount of black body radiation, an infra-red camera can detect this in the same way an ordinary camera detects visible light. For use in temperature measurement the brightest parts of the image are coloured white and indicate a hot zone, where blues and blacks indicate a cold zone (Figure 6). This was used in this project briefly to obtain images of the room and of humans to validate temperature profiles obtained by CFD. Whilst the thermography only receives infrared, it is able to tell us core temperatures from this, which can be directly compared to object temperatures.

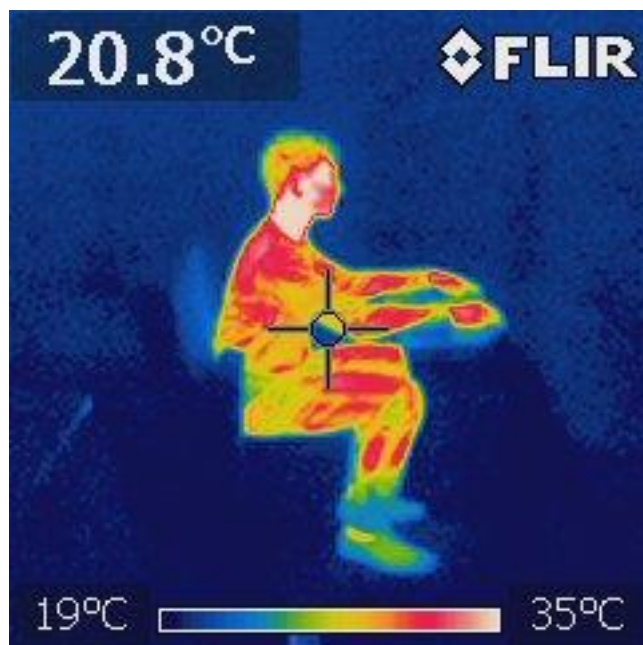


Figure 6 – Example Thermal Image of Group Member

5. Methodology and Design

As mentioned in the introduction to the report, the work was split up into three key sections. The room group was made up of Locci, Smith and Bunting. As was decided earlier in the project, Harrison Room 170 was chosen as the test bed for the simulations. Locci assumed the role of setting up a detailed model of the room which included fluid flow as well as heat transfer [32]. He then went on to work in conjunction with myself to incorporate the human into the room. Smith took the work previously carried out by Loomans et al. and investigated it further, before taking his findings and contributing to the Room 170 work [17]. He also used this work to investigate different ventilation systems for the built environment. Bunting initially worked alongside Locci and Smith developing the Room 170 geometry, before investigating the Lumped Parameter Model [33]; a theoretical model which simulates a given built environment as a circuit. This uses resistors and capacitors to represent walls and heat sources respectively. The electronics group also made use of the Room 170 test bed, with the intention of setting up temperature and humidity sensors in it. Katrina Pamatmat designed and calibrated sensors [34], whilst Dalladay-Simpson worked on connecting them all up to feed data back to the loggers in the room [35]. The human group comprised of Tompsett and myself. Tompsett focused on a vase shaped geometry, producing a highly accurate mesh and CFD simulation, before incorporating it into Locci's room model [36]. My role was to generate a simplistic geometry and model it accurately in CFD before coupling it with the Fiala human comfort model. Work was then done with Locci to couple the human and the room together.

5.1. Initial Design Work

As mentioned above, this part of the project looked at the human aspect. The first task was to generate a human geometry to work with.

5.1.1. Solidworks Design

Working alongside Tompsett, the figure displayed in Figure 7 was generated. Made up of a series of lofts, cylinders and spheres, the geometry represents a very simple human shape. Roughly 1.75m tall the geometry was based on an average British Male in order to accurately represent humans as well as possible. As can be seen, the geometry is very simple with no facial features or fingers. This is due to the extra level of detail required to mesh these areas, when the output differences are likely to be very small. It will also reduce the required computational power.

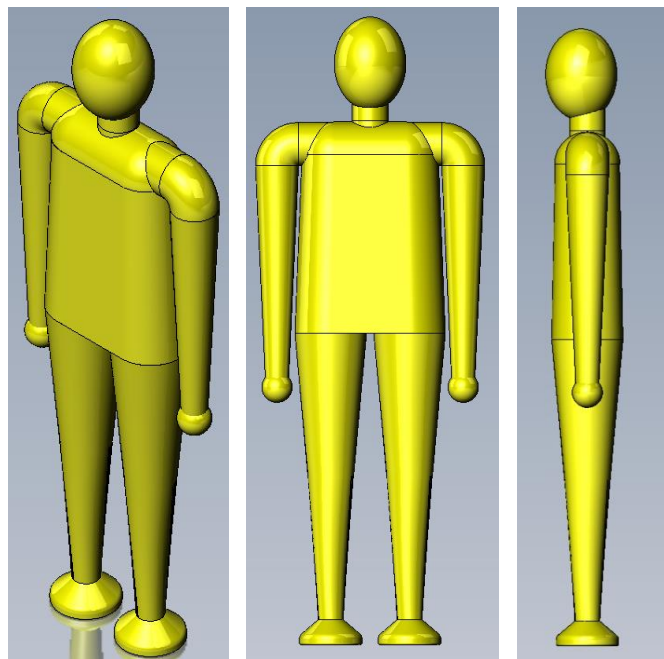


Figure 7 – Simple Human Geometry Generated on Solidworks

5.1.2. David Laserscanner

The other option when generating human geometry was to scan a member of the group, convert it into a CAD file and simulate it in ANSYS. However, this proved more difficult than first thought. Due to financial constraints as well as time, the equipment bought for this task was not the most advanced available. In order to fully use the potential of David Laserscanner software, or indeed any laser scanning, a test rig with powerful lasers and an advanced camera would be required. None-the-less, scanning was attempted on a smaller scale. In order to do this the following items were bought on the project budget or required:

- Red Laser Line, 5mW, Battery-Operated, 90° CLASS 1 - £24 + VAT
- Logitech Webcam C525 - £34
- Calibration Panels
- David Laserscanner Software – Free Download

Due to health and safety reasons, it was required that the laser was in the class one category, meaning it is eye safe. This limited performance but still produced some results. The camera was calibrated using two printed pieces of paper which were placed at 90° to each other in front of the camera. Once calibrated, the light and exposure were adjusted until only the laser line was visible on screen. Once this was set up, an art manikin was placed in front of the camera for scanning. Figure 8 shows the setup of the program as well as the scans that were produced. As can be seen around twelve scans were taken and the shape fusion capabilities of the software were used to create a fused model. The scanned model is incomplete, perhaps because the laser was too weak, or because some of the faces were not reflective enough. For example some dark faces may absorb the light and not reflect it back for the camera to read. As this was only on a small scale, it was clear that with the apparatus available to us, it would not be possible to scan a full human. To do this, a room would be required containing a rig and a more capable camera. Another issue associated with scanning a live human is the movement of the human. When the software matches up the scans to one another, it assumes all the shapes are the same. Otherwise one face may match up and the others may not, producing an inaccurate model. To fully scan a human from many angles whilst maintaining the same shape would require apparatus to hold the body in the same position. For the reasons stated above, the decision was made to go forward with the model generated on Solidworks. This would also be easier to work with inside ANSYS with only a small number of known faces.

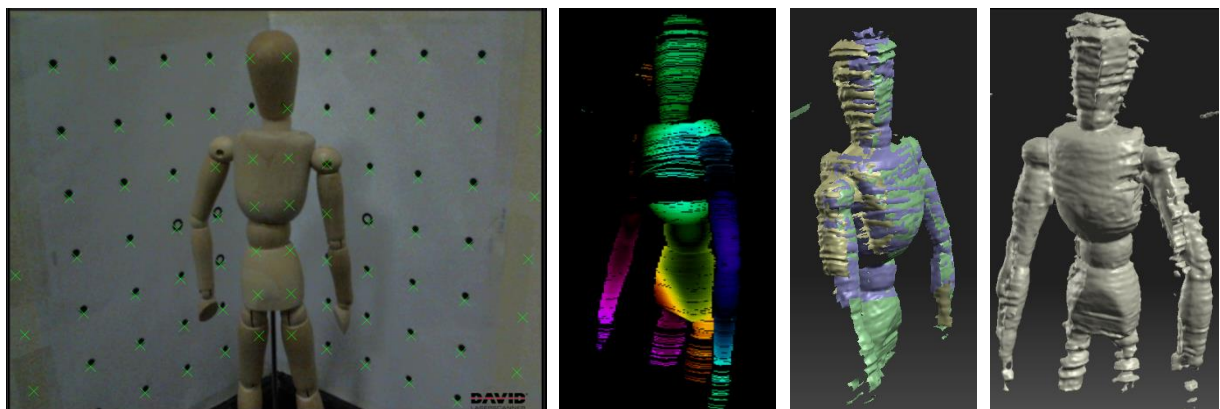


Figure 8 – David Laser Scanning Process Including Calibration, Scanning, Aligning Scans and Fusion

5.2. Preliminary Heat Transfer Simulations

In order to understand how to perform heat transfer simulations in Fluent, a simplistic case was first set up. With the intention purely to see a thermal plume, a basic cylinder was placed in a controlled volume and given a constant temperature. This is displayed below in Figure 9.

Setting up the model correctly ensured that the future simulations would be modelled with the correct settings. This meant turning on the correct turbulence model, the Boussinesq approximation, gravity and setting up the correct boundary conditions. To represent natural ventilation, the control volume was modelled as a wall, with two zero velocity inlets and two zero pressure outlets. These allowed air to flow in and out of the box without having an effect on the pressure or recirculation. To enable the Boussinesq approximation, the density of air at 20°C was used as ρ , and the thermal expansion coefficient β was also entered; $3.43 \times 10^{-5} \text{ K}^{-1}$. This allowed for buoyancy driven flow to be modelled in the desired conditions, as described in the theory.

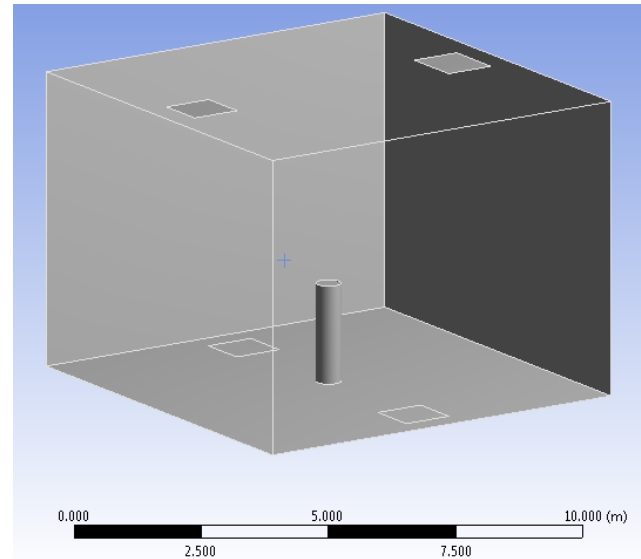


Figure 9 – Basic Cylinder Setup

The mesh was generated with 440,425 cells so there was a moderate level of accuracy. As can be seen in Figure 10 below, natural convection is visible with raised temperatures around and above the cylinder. This validates that the heat transfer model being used is producing acceptable results. The next step would be to model heat transfer with the chosen geometry, before incorporating the human comfort model as well.

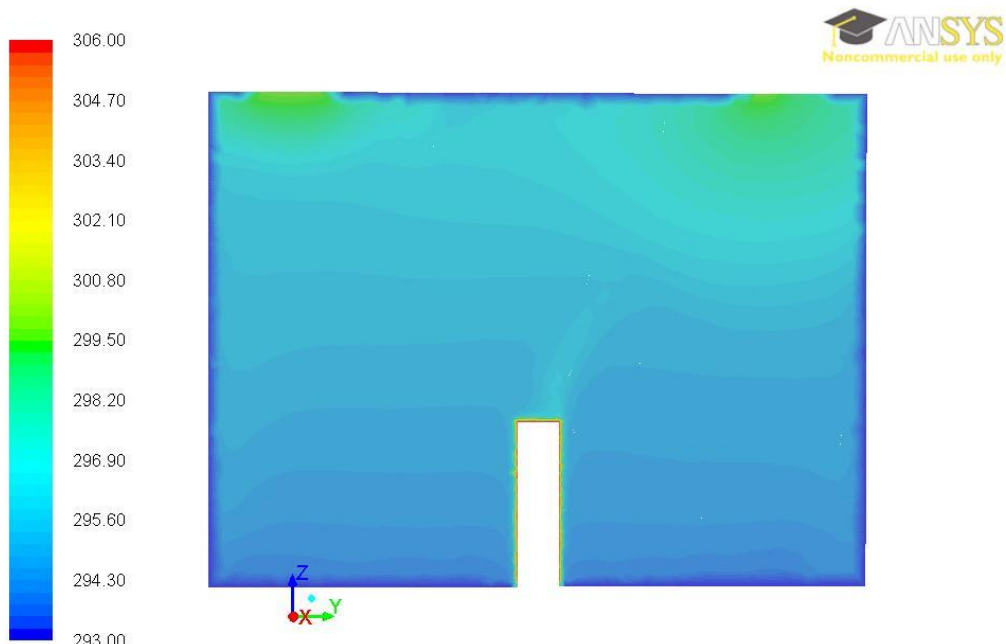


Figure 10 – Temperature Contours across Midplane (K)

5.3. Using the IESD-Fiala Model

The Fiala model is free to download with permission from the author, as previously mentioned. It works by running an executable file that reads a number of text files stored within the key directories. The parent folder contains four main directories: BCFILES which contains files describing the boundary conditions, CLO which contains text files describing the clothing model, HELP which contains all relevant information on how to use the model, and OUTPUTS which contains a number of text files generated once the executable file has been run. It also contains a configuration file named Cfg324.txt containing relevant information from the other directories, and the executable file HDT3.exe used to run the model.

time	Ta	Twall	va	rh	activ
[min]	[°C]	[°C]	[m/s]	[]	[met]
-60	28.00	28.00	0.10	30.00	1.80
-40	28.00	28.00	0.10	30.00	1.80
-20	28.00	28.00	0.10	30.00	1.80
-3	28.00	28.00	0.10	30.00	1.80
0	43.00	42.00	0.12	30.00	1.00
5	43.00	42.00	0.12	30.00	1.00
10	43.00	42.00	0.12	30.00	1.00
15	43.00	42.00	0.12	30.00	1.00
20	43.00	42.00	0.12	30.00	1.00
25	43.00	42.00	0.12	30.00	1.00

Figure 11 – Example BC File

Figure 11 shows an example boundary condition file. The parameters shown in this file are the conditions that the human is exposed to. It consists of time (min), ambient temperature (°C), wall temperature (°C), air velocity (m/s), relative humidity (%) and activity level (met). These conditions can change throughout the file, and the model will accurately predict the body's response. The time steps can be reduced for more precision and it can simulate up to a number of hours.

The clothing of the human is specified with files in the CLO directory. Each file contains a different clothing setup, which contains data for each body part and whether it is covered or not. For the most part of this work, a male in briefs is modelled, although other models are looked at to compare thermal contours.

With the boundary condition file setup correctly for the simulation, and the correct clothing file selected, the configuration file is edited to contain these before the executable file is run.

```

1 -----
2 ----- Configuration File 3.23 -----
3 -----
4 I) Boundary Conditions File:
5 a) Filename:
6
7 BCFILE1.TXT
8
9 b) number of headlines in BF-file: min.=0, max.=5)
10 2
11
12 c) number of air temperatures included in BC-file:
13 1      (max. 1)
14
15 d) number of air velocities included in BC-file:
16 1      (max. 1)

```

Figure 12 – Example Configuration File

A small section of the configuration file is displayed above in Figure 12. Line 7 contains the boundary condition file name to be read. Further down the list it contains the clothing file name to be read as well. It also contains details of each file it is reading, so that each line of each text file is read correctly. Once the configuration file is saved, the executable file can be run (Figure 13).

```
t=944min Tskm=30.9°C Thy=37.4°C Qm=212W Esk= 28W SkBF= 37% DTS=-0.4 PPD= 8.6%
t=946min Tskm=30.9°C Thy=37.4°C Qm=212W Esk= 28W SkBF= 37% DTS=-0.4 PPD= 8.6%
t=948min Tskm=30.9°C Thy=37.4°C Qm=212W Esk= 28W SkBF= 37% DTS=-0.4 PPD= 8.6%
t=950min Tskm=30.9°C Thy=37.4°C Qm=212W Esk= 28W SkBF= 37% DTS=-0.4 PPD= 8.6%
t=952min Tskm=30.9°C Thy=37.4°C Qm=212W Esk= 28W SkBF= 37% DTS=-0.4 PPD= 8.6%
t=954min Tskm=30.9°C Thy=37.4°C Qm=212W Esk= 28W SkBF= 37% DTS=-0.4 PPD= 8.6%
t=956min Tskm=30.9°C Thy=37.4°C Qm=212W Esk= 28W SkBF= 37% DTS=-0.4 PPD= 8.6%
t=958min Tskm=30.9°C Thy=37.4°C Qm=212W Esk= 28W SkBF= 37% DTS=-0.4 PPD= 8.6%
t=960min Tskm=30.9°C Thy=37.4°C Qm=212W Esk= 28W SkBF= 37% DTS=-0.4 PPD= 8.6%
t=962min Tskm=30.9°C Thy=37.4°C Qm=212W Esk= 28W SkBF= 37% DTS=-0.4 PPD= 8.6%
t=964min Tskm=30.9°C Thy=37.4°C Qm=212W Esk= 28W SkBF= 37% DTS=-0.4 PPD= 8.6%
t=966min Tskm=30.9°C Thy=37.4°C Qm=212W Esk= 28W SkBF= 37% DTS=-0.4 PPD= 8.6%
t=968min Tskm=30.9°C Thy=37.4°C Qm=212W Esk= 28W SkBF= 37% DTS=-0.4 PPD= 8.6%
t=970min Tskm=30.9°C Thy=37.4°C Qm=212W Esk= 28W SkBF= 37% DTS=-0.4 PPD= 8.6%
t=972min Tskm=30.9°C Thy=37.4°C Qm=212W Esk= 28W SkBF= 37% DTS=-0.4 PPD= 8.6%
t=974min Tskm=30.9°C Thy=37.4°C Qm=212W Esk= 28W SkBF= 37% DTS=-0.4 PPD= 8.6%
t=976min Tskm=30.9°C Thy=37.4°C Qm=212W Esk= 28W SkBF= 37% DTS=-0.4 PPD= 8.6%
t=978min Tskm=30.9°C Thy=37.4°C Qm=212W Esk= 28W SkBF= 37% DTS=-0.4 PPD= 8.6%
t=980min Tskm=30.9°C Thy=37.4°C Qm=212W Esk= 28W SkBF= 37% DTS=-0.4 PPD= 8.6%
t=982min Tskm=30.9°C Thy=37.4°C Qm=212W Esk= 28W SkBF= 37% DTS=-0.4 PPD= 8.6%
t=984min Tskm=30.9°C Thy=37.4°C Qm=212W Esk= 28W SkBF= 37% DTS=-0.4 PPD= 8.6%
t=986min Tskm=30.9°C Thy=37.4°C Qm=212W Esk= 28W SkBF= 37% DTS=-0.4 PPD= 8.6%
t=988min Tskm=30.9°C Thy=37.4°C Qm=212W Esk= 28W SkBF= 37% DTS=-0.4 PPD= 8.6%
t=990min Tskm=30.9°C Thy=37.4°C Qm=212W Esk= 28W SkBF= 37% DTS=-0.4 PPD= 8.6%
t=992min Tskm=30.9°C Thy=37.4°C Qm=212W Esk= 28W SkBF= 37% DTS=-0.4 PPD= 8.6%
t=994min Tskm=30.9°C Thy=37.4°C Qm=212W Esk= 28W SkBF= 37% DTS=-0.4 PPD= 8.6%
t=996min Tskm=30.9°C Thy=37.4°C Qm=212W Esk= 28W SkBF= 37% DTS=-0.4 PPD= 8.6%
t=998min Tskm=30.9°C Thy=37.4°C Qm=212W Esk= 28W SkBF= 37% DTS=-0.4 PPD= 8.6%
t=1000min Tskm=30.9°C Thy=37.4°C Qm=212W Esk= 28W SkBF= 37% DTS=-0.4 PPD= 8.6%
Copyright <c> 1998-2004
De Montfort University
... press Enter
```

Figure 13 – Executonal File Run to simulate 1000 minutes

Once this file has been closed, a prompt is sent to generate multiple results files. Data for the following outputs is produced [37]:

- Heat transfer coefficients and resistances
 - hc = Local surface convective heat transfer coefficients ($\text{W/m}^2/\text{K}$)
 - hr = Local surface long-wave radiant heat transfer coefficients ($\text{W/m}^2/\text{K}$)
 - Rcl = Local clothing resistances (clo)
 - Recl = Local clothing evaporative resistances ($\text{m}^2\text{Pa}/\text{W}$)
- Heat transfer rate
 - qcnd = Local conductive heat fluxes (W/m^2)
 - qcnv = Local convective heat fluxes (W/m^2)
 - qEv = Local evaporative heat fluxes (W/m^2)
 - qLwR = Local long-wave radiant heat fluxes (W/m^2)
 - qSwR = Local short-wave radiant heat fluxes (W/m^2)
 - qsk = Local total heat fluxes (W/m^2)
 - Qsk_ = Local skin total heat losses (W)
- Sweat and Evaporation
 - msw = Local sweat production rates (g/min)
 - psk = Local vapour pressures at skin surface (Pa)
 - RHsk = Local relative humidity at skin surface (%)
 - wsk = Local skin wettedness
 - accMsk = Local accumulated moisture at skin surface (g)

- Temperature
 - Tcore = Core temperature of each body part ($^{\circ}\text{C}$)
 - Tsk = Local skin temperature ($^{\circ}\text{C}$)
 - TskL&R = Local skin temperature (unsymmetrical) ($^{\circ}\text{C}$)
 - Tclo.txt = Local cloth temperature (unsymmetrical) ($^{\circ}\text{C}$)
- Physiological
 - blood = Local blood circulation (ml/min) and artery/vein temperatures ($^{\circ}\text{C}$)
 - wblsk = Local skin blood perfusion rates (% Basal)
- Comfort and Results
 - CMF = Body thermal state variables and comfort
 - CmfPrm = Environmental condition variables and comfort
 - TRS = Thermal regulatory variables
 - GICalVar = Global operative temperatures and heat losses
 - GIResults = Global environmental, physiological, regulatory, and comfort variables
 - results = Global physiological and regulatory results

Data for each of the above outputs is generated for each of the 59 faces of the body. These are displayed below in Table 2 along with their respective areas. In order to observe how the surroundings respond to the human, the main outputs to be used were skin and clothing temperatures. From these natural and forced convection could be modelled.

Table 2 – Faces the Human is Split into by the Fiala Model and their Respective Areas [37]

Body part	Side	Area [m ²]	Body part	Side	Area [m ²]
Whole body		1.85042	Upper arm	anterior	0.01843
Head	Forehead	0.00604		posterior	0.01819
	back of head	0.06192		inferior	0.01245
Face	anterior	0.01313		exterior	0.03711
	exterior left	0.00750	Lower arm	anterior	0.00987
	exterior right	0.00750		posterior	0.01323
Neck	anterior	0.00483		inferior	0.02870
	posterior	0.00667		exterior	0.02893
	exterior left	0.00925	Hand	back	0.02238
	exterior right	0.00925		palm	0.02164
Shoulder	exterior	0.01670	Upper leg	anterior	0.03399
				posterior	0.02826
Thorax	anterior	0.11368		inferior	0.02969
	posterior	0.10265		exterior	0.03685
	inferior left	0.01585	Lower leg	anterior	0.02086
	inferior right	0.01585		posterior	0.03037
Abdomen	anterior	0.16145		inferior	0.02731
	posterior	0.15902		exterior	0.03191
	inferior left	0.05827	Foot	upper	0.03504
	inferior right	0.05827		lower	0.01774

5.4. Split Human

As a large part of this project looks at coupling the human geometry with the Fiala model, it was important that the human geometry was set up in a way that the model could be incorporated. In a similar way to Cropper et al., it was decided that the human geometry from Solidworks would be split up into a number of faces which correspond with the output files from the IESD-Fiala model. As mentioned above, the Fiala model outputs data for 59 different faces. Therefore, the human geometry was split up to match these. Due to complications when importing geometries into ANSYS from Solidworks, the splitting of faces was carried out in the ANSYS Geometry Modeller. This was achieved by generating a number of lines and points, before using the “face split” tool to separate them. The split geometry can be seen in Figure 14 below.

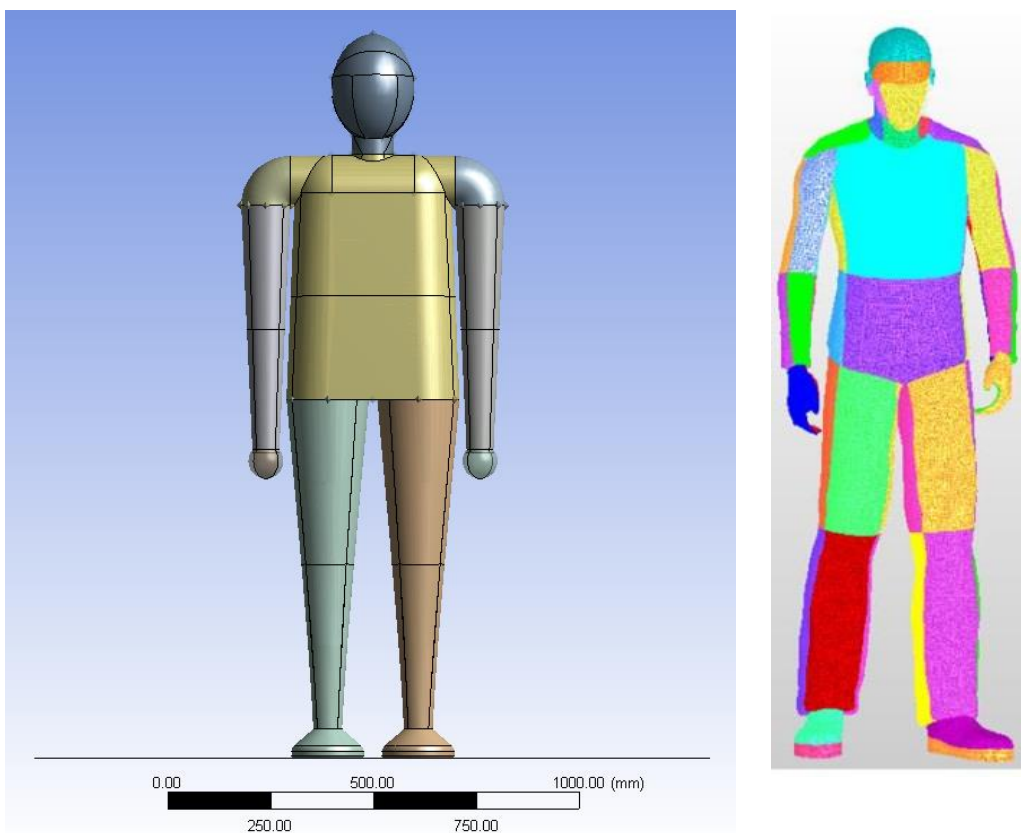


Figure 14 – Solidworks Human Geometry Split into Faces compared with Split Model by Cropper et al. [14]

The split geometry of Cropper et al. is also displayed in Figure 14 for comparison purposes. Whilst the faces in the simple model are more basic, they still roughly line up in terms of area with those of Cropper et al., and they all have a corresponding face from the Fiala outputs. Cropper et al.’s model contains clothing, whereas the simple model does not due to difficulty in modelling and time constraints. However, as clothing can be modelled inside the Fiala model, the surfaces can be given either skin or clothing temperatures depending on how the Fiala boundary condition file is specified. Each face was then given a named selection in the meshing module, so that boundary conditions could be applied separately to each one.

5.5. Free Convection Human Geometry

Once the human was arranged into faces, an initial simulation was run. Assuming certain conditions for the Fiala model, skin temperature outputs were used as boundary conditions on the body surface. To provide accurate results, the detailed mesh displayed in Figure 15 was used. The cutcell assembly mesh method was utilised, with face sizing of 0.005m applied to all of the human faces. Inflation was also used with a growth rate of 1.2, creating a mesh with 822,330 cells.

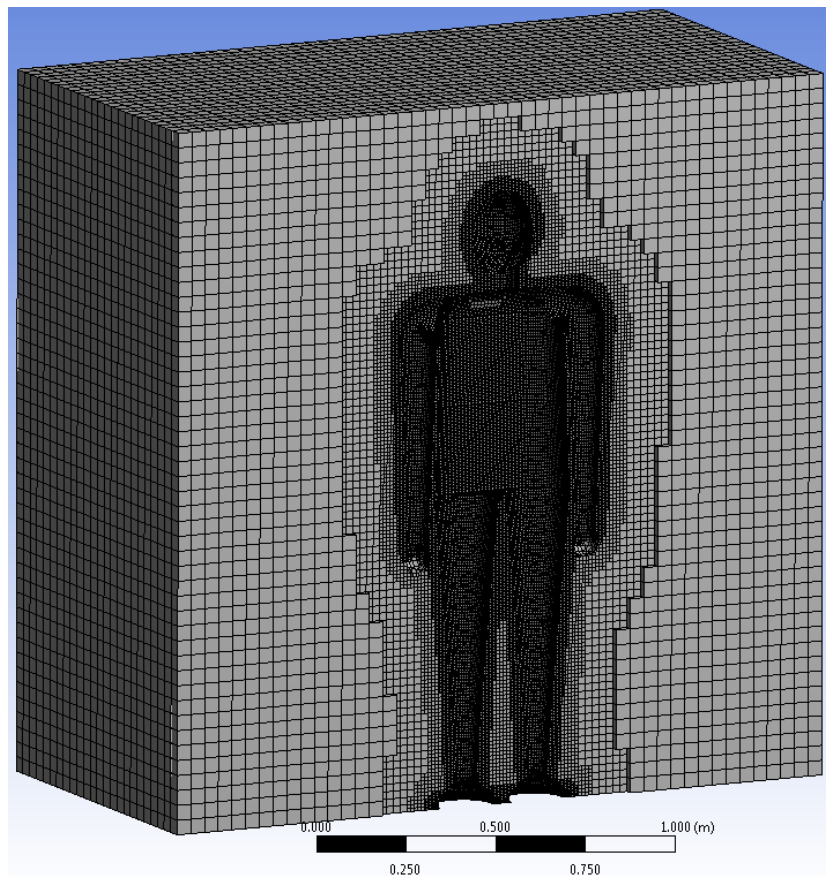


Figure 15 – Detailed Mesh with Surface Sizing

First of all, the geometry was set up with all of the body faces modelled as walls. All of the side faces and the floor were modelled as walls and the top face was modelled as a pressure outlet. As described earlier, the Boussinesq model was used, as was the K-Omega SST turbulence model. The boundary conditions included face temperatures from the Fiala output and walls at a constant temperature of 20°C. This was achieved by running the Fiala model for 1000 minutes, until convergence was achieved. This was checked by plotting variables for each time step in MS Excel. Once converged, the values from the final time step were entered manually as surface temperatures in fluent. The simulation was set up to run for 1000 iterations or until the residuals converged. Convergence is paramount in CFD as it explains whether the simulation is successful or not. If the residuals diverge, the data will be inaccurate. Once the calculation was complete the following contours and vectors were displayed to illustrate the flow behaved in the domain (Figure 16 and Figure 17).

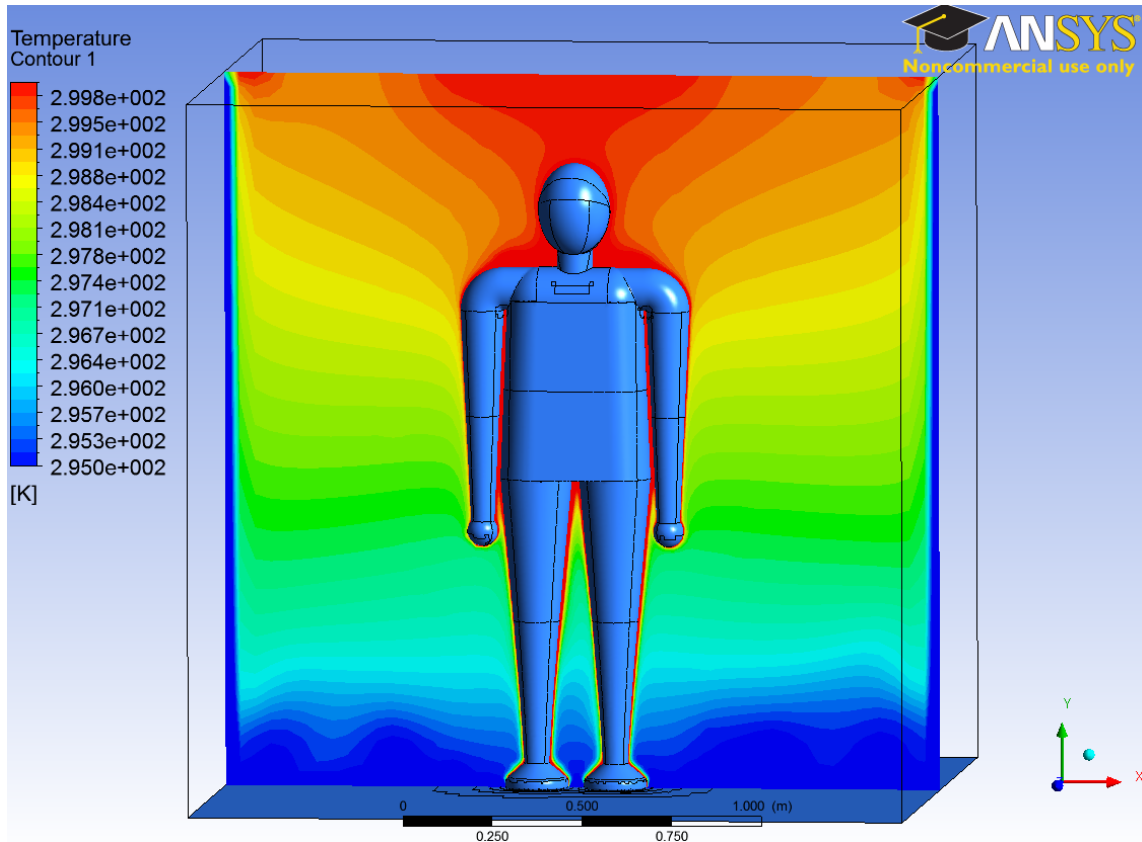


Figure 16 – Temperature Contours of Male in Briefs

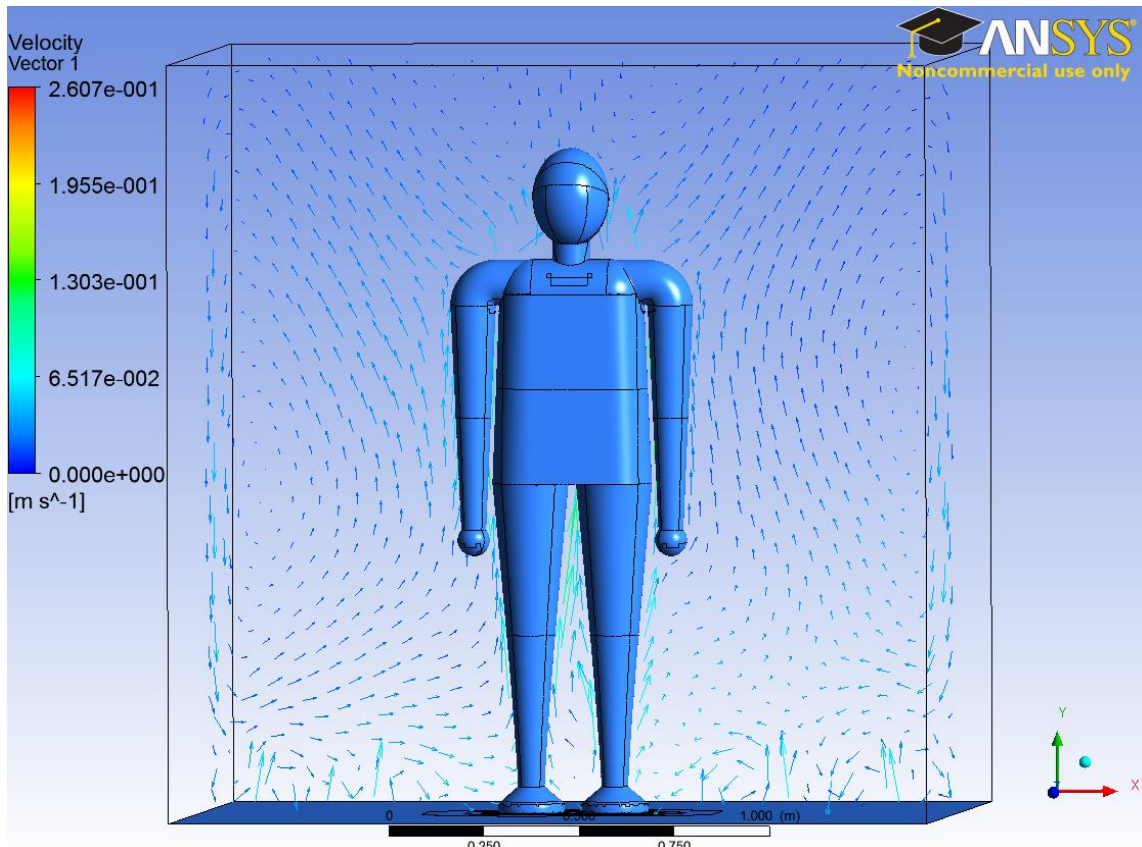


Figure 17 – Velocity Vectors of Male in Briefs

The Fiala model was run with the ambient temperature set at 25°C, with the human wearing briefs. The skin temperatures produced a visible thermal plume ranging from 295K (wall temperature) to 299K (maximum air temperature above human). The contours displayed above were generated using the ANSYS post CFD module. The temperature clearly rises with a relatively wide plume, as almost all of the body is a similar temperature. As expected the lower half of the room is coldest as the heated air rises. The reason for a relatively constant temperature gradient from the floor upwards is due to the lack of ventilation from the floor. The only way air is retained at the bottom is by recirculation, which can be seen from the velocity vectors in Figure 17. The vectors clearly show that beside the body, the air is rising, whilst it sinks nearer the walls to fill the gaps left by the hot air. After enough time, this causes the temperature gradient to level out as the air mixes with itself. The same simulation was run again, but using a separate clothing file CloA which means the body was wearing trousers, a top and shoes. With all areas of the body covered apart from the head, neck and hands, the thermal plume was expected to be narrower. This is because most of the heat should come from the head, as the rest of the body should have cooler surfaces. As the Fiala outputs clothing surface temperatures as well as skin, these were used as the boundary conditions. Figure 18 shows the temperature contours for the human with full clothing.

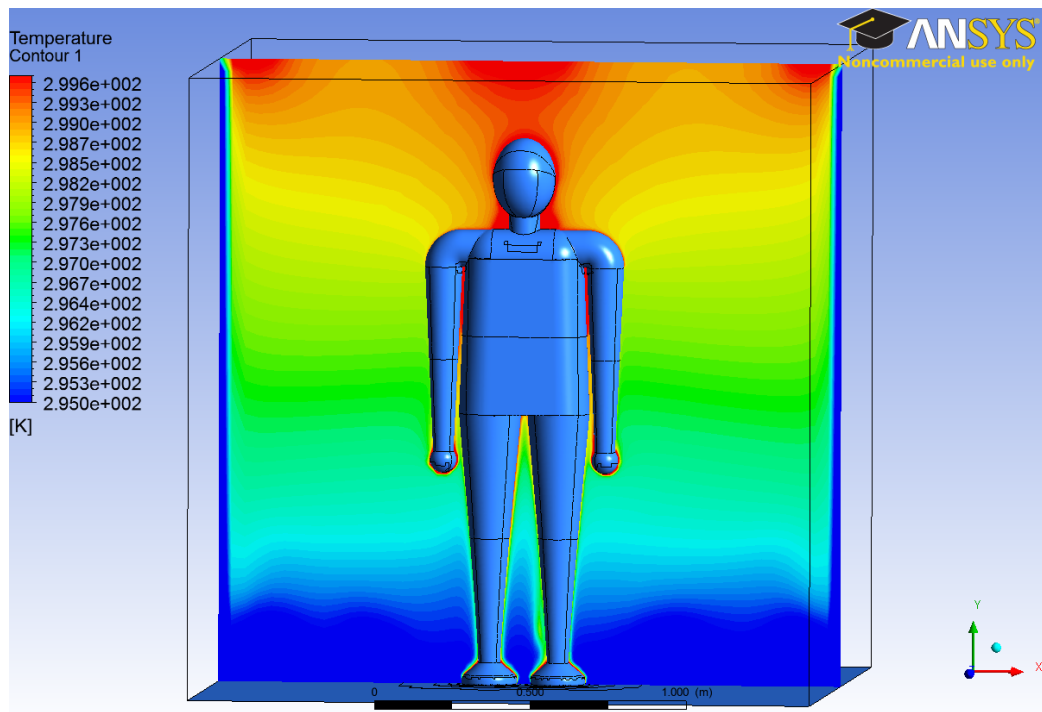


Figure 18 – Temperature Contours of Male in Full Clothing

As expected, the thermal plume is narrower suggesting the model worked correctly. Again the temperature gradient is constant from the floor upwards for the same reason. These initial simulations were run to obtain visible natural convection, which was achieved. To simulate natural ventilation, the set up was modified to include vents at the top and bottom, in order to create only hot air around and above the human.

In order to couple the CFD model with the Fiala model, it was important to set up the CFD case correctly. The coupling would be done in a way that the Fiala model is run with boundary conditions. The Temperature outputs would then be used as temperature boundary conditions in the CFD model. After running the CFD model until convergence, the new ambient temperature would be measured and used as the new ambient temperature in the Fiala model. In theory the human should heat up the room, which should cause the human to heat up further, and so on. Eventually a convergence should be reached where the effect of one on the other becomes minimal. The new setup consisted of a volume 2m x 2m x 2m with four inlet vents on the bottom face and two outlet vents on the top face (Figure 19). All other faces were modelled as walls with constant temperatures.

Initially, the same quality mesh was used as in Figure 15 to obtain some initial results. Unfortunately this mesh failed to converge, with issues most likely occurring due to mesh detail at the inlets and outlets. In an attempt to successfully run the simulation, extra detail was added to the vents, as well as to the walls, and a mesh convergence study was used to find the optimum mesh. Due to the flow occurring near the walls, the mesh in these areas may have been preventing the simulation from running successfully.

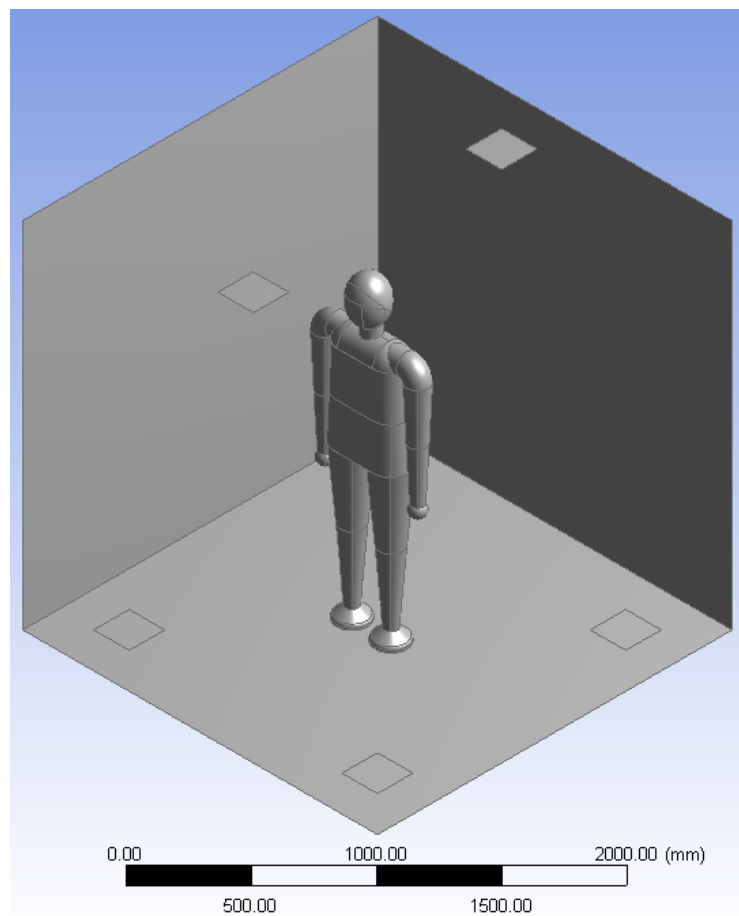
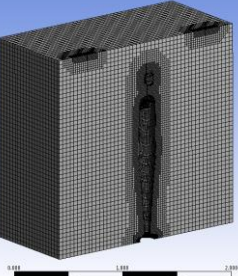
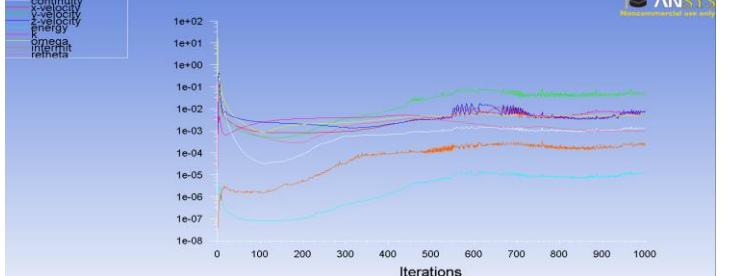
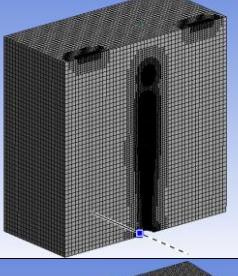
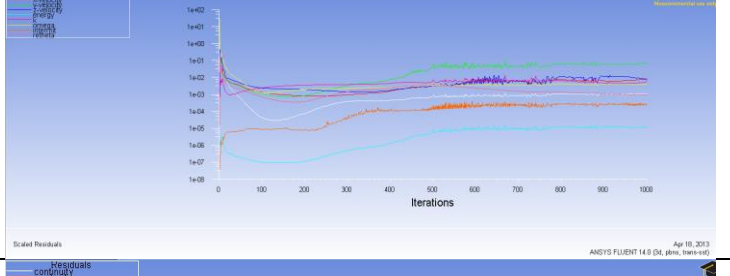
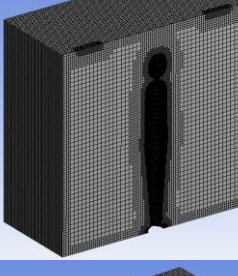
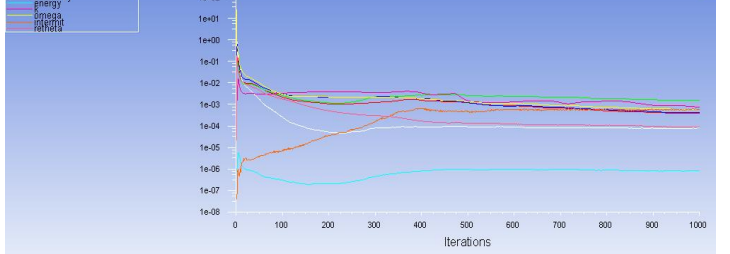
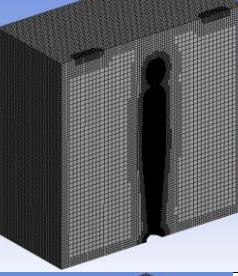
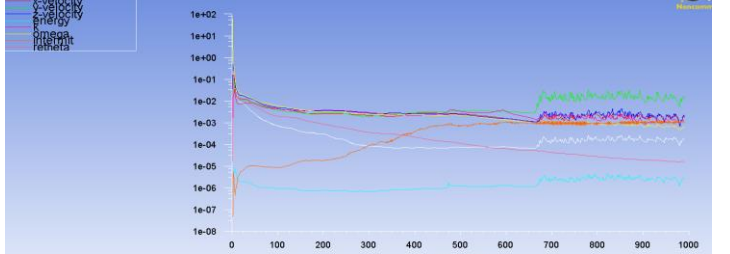
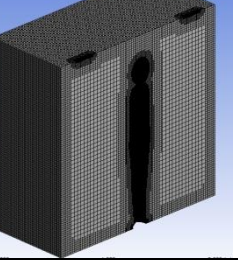
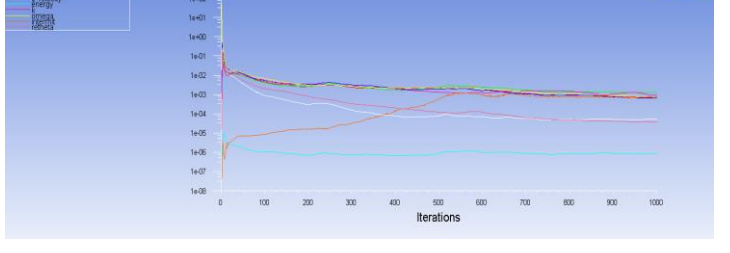


Figure 19 – Setup of Volume with Vents

5.6. Mesh Convergence Study

The eventual mesh to be used for coupling was chosen from a mesh convergence study. This meant running the same simulation for a number of meshes until the level of detail no longer impacted the results of the calculation. Table 3 shows how the residuals converged for each mesh.

Table 3 – Details of the Mesh Convergence Study

Number of Cells	Visual Mesh	Residual Convergence
380,710		 <p>Residuals: Continuity, X-velocity, Y-velocity, Energy, Omega, Intensity, Reheat</p> <p>Iterations: 0 to 1000</p>
665,592		 <p>Residuals: Continuity, X-velocity, Y-velocity, Energy, Omega, Intensity, Reheat</p> <p>Iterations: 0 to 1000</p>
960,654		 <p>Residuals: Continuity, X-velocity, Y-velocity, Energy, Omega, Intensity, Reheat</p> <p>Iterations: 0 to 1000</p>
2,202,569		 <p>Residuals: Continuity, X-velocity, Y-velocity, Energy, Omega, Intensity, Reheat</p> <p>Iterations: 0 to 1000</p>
2,766,469		 <p>Residuals: Continuity, X-velocity, Y-velocity, Energy, Omega, Intensity, Reheat</p> <p>Iterations: 0 to 1000</p>

The final mesh contained face sizing at the body faces of 0.003m, at the vents of 0.008m and at the walls of 0.02m. This highly detailed mesh was made up of roughly 2.77 million cells and ran successfully for 1000 iterations. As can be seen from Table 3 above, the residuals steadily improve with an increase in cells and refinement. Strangely the residuals in mesh four seem to oscillate after around 700 iterations. However, refining the mesh even further removed this problem. As well as checking residuals, data values were taken from each mesh to ensure the solutions were converging to a similar value. In this instance, maximum values for velocity and dynamic pressure were recorded from the midplane.

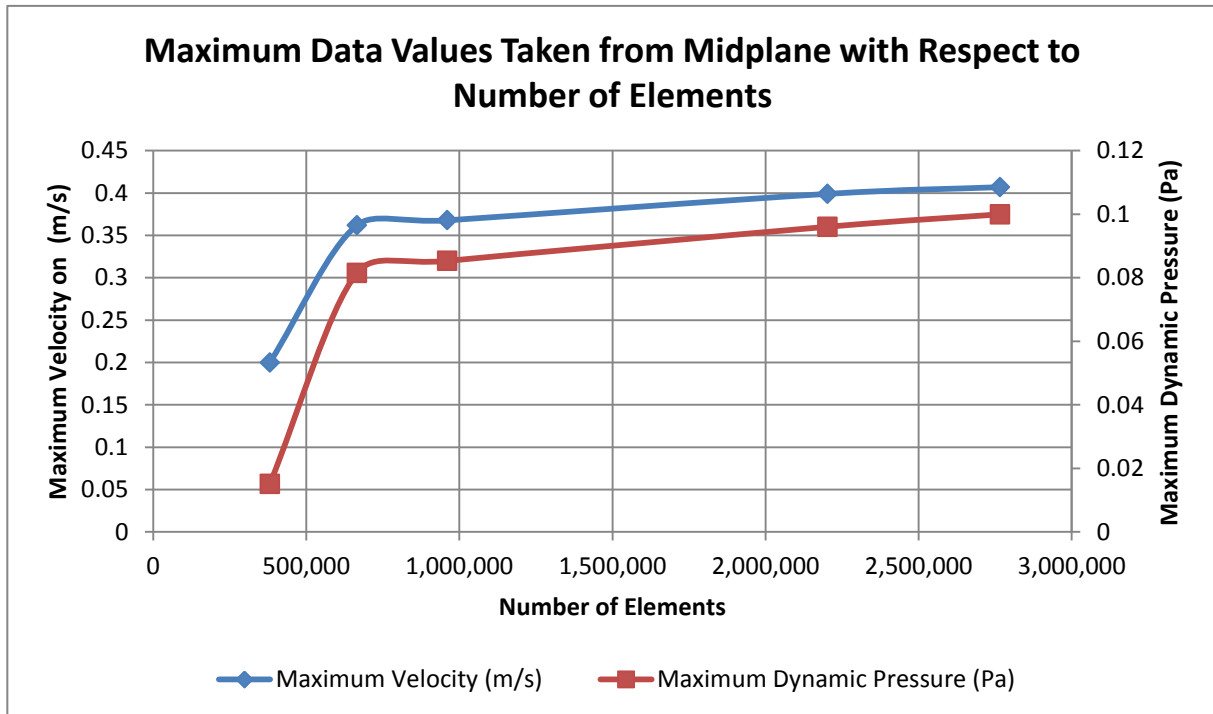


Figure 20 – Data Values from Midplane to Display Mesh Convergence

Figure 20 shows that values for maximum pressure and maximum velocity both converged with mesh refinement. Adding further detail to the mesh would result in a very small change in accuracy, therefore the computational power and time is not justified. For that reason, the fifth mesh was used for further investigation. Further details on the mesh refinement can be seen in Appendix B.

5.7. Free Convection Coupling

Having refined the mesh in order to produce accurate results, the next step in the process was to couple the Fiala comfort model with the CFD simulation to predict how the human affects the surroundings over time. To do this, an initial Fiala simulation was run with a boundary condition stating an ambient temperature of 20°C, air velocity of 0 m/s, an average humidity level of 30%, and an activity level of 2 met. This essentially works as if the human enters into a small room with only natural ventilation, with no additional heat sources, and stands in the centre. The Fiala model was run for an extended period of time of 1000 minutes. The reason for this is it allows the solution to reach a steady state convergence. This effectively acts as though a human is in a room indefinitely with constant temperatures until the body's

responses no longer change i.e. it has stabilised. Of course this is not entirely accurate, as the surroundings would change. This is therefore taken into account by the CFD model, which is also run until steady state convergence. The converged temperatures from the CFD are taken as the new ambient temperature for the second Fiala run, whose outputs are re-entered as boundary conditions to the CFD and so on. With both models running steady state, the two way data transfer should eventually lead to a convergence between the two, with the resultant temperatures in the room changing less and less each time. The steady state method seems the most accurate way of measuring the eventual change in environment. Other methods would look at transient simulations, but this would require feeding results from the Fiala after every time step and vice versa, which would become very complicated.

Step 1

Fiala Model was run for 1000 minutes (convergence displayed in Figure 21) with the following conditions:

- Ambient Temperature = 20°C
- Wall Temperature = 20°C
- Ambient Velocity = 0°C
- Activity Level = 2 met
- Humidity = 30%

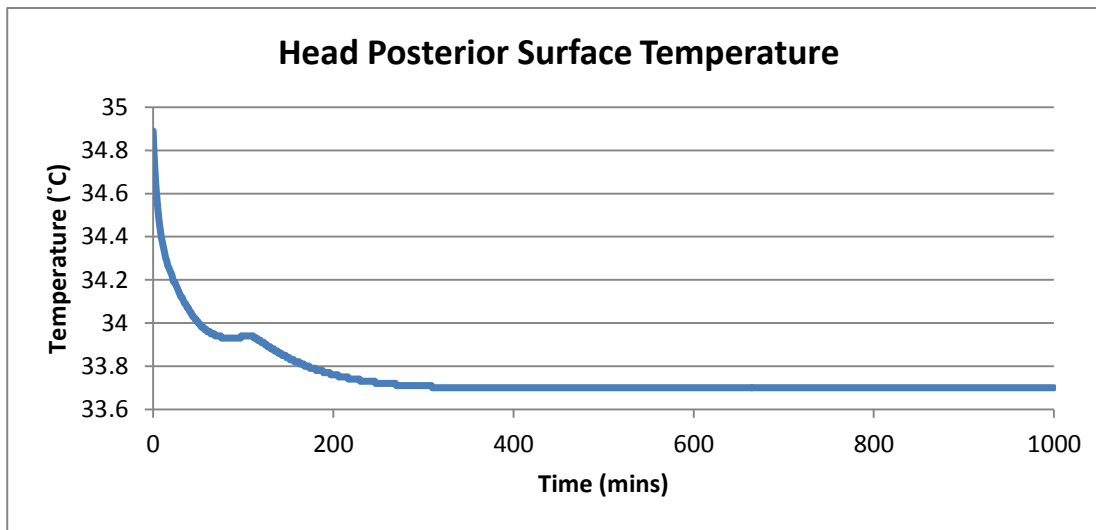


Figure 21 – Example Temperature Convergence from Fiala Output Files

Step 2

CFD steady state simulation was run for 1000 iterations or until convergence under the following conditions:

- Fiala output temperatures used as skin temperature boundary conditions
- Walls = 20°C constant temperature
- Buoyancy modelled using Boussinesq approximation
- Solution Method: 2nd Order Pressure Discretisation

Step 3

Fiala Model was run again for 1000 minutes with new conditions found by averaging temperature values across the mid-plane. The new conditions were as follows:

- Ambient Temperature = 21.659°C

Step 4

Repeat step 2 with new temperatures.

This process was continued until the solution converged. Once convergence was reached, the visualisations and data shown in section 6.1 were recorded in order to analyse how the human affected the room after an extended time period.

5.8. Coupling within Room 170 Model; Working with Gianluca Locci

Having used the coupling process on the free convection case, it was now possible to transfer this knowledge across to the larger scale group aim of the project. This was to incorporate the human into the chosen room, Harrison 170.

Using the model generated by Gianluca Locci [32], the human was added in Solidworks before being imported into ANSYS. In order to reduce the complexity slightly as well as making the process more time efficient, the body was split into fewer faces: torso, back, sides, arms, legs, hands, feet, neck, face and head. To simulate a realistic human in the room, all Fiala calculations were run using a clothing file which covered all of the body bar the head, hands and neck. With the human standing at the front of the room, representing a lecturer, the model was first run to obtain starting values. This meant running the simulation without the human as a heat source. All other heat sources were turned on, such as the computer and projector, as well as the air conditioning. The human surfaces were therefore set as symmetry conditions, meaning they act in a similar way to walls without affecting the temperature or pressure of the flow. Running it this way was effectively taking the room conditions before the human enters. After convergence of the initial simulation, the ambient temperature was recorded. This was achieved by creating a surface of revolution around the human. On this surface, contours of temperature were plotted, and the area average was calculated using the expression feature in CFD-Post. This allowed an accurate average of the immediate surroundings to be recorded and used as the ambient temperature for the Fiala model. As well as temperature, velocity was recorded as this room included air conditioning. Humidity was assumed to be 30% and an activity level of 2 MET was used (standing).

The results for this study can be viewed in section 6.2 and further details of the setup of the room can be found in Appendix D and the report of Locci [32].

6. Results

6.1. Free Convection Coupling

Coupling together the IESD Fiala model and the CFD simulation produced an iterative process that predicted the human's effect on the local environment over an extended period of time. As expected, the rise in temperature in the room due to the human's presence caused the human to respond by heating up. This was shown from the new Fiala outputs, displaying higher skin temperatures. This again caused a rise in room temperature, although with slightly less impact. As the two processes combined, the results converged until no further differences were visible, i.e. a steady state result was achieved. This is displayed in Figure 22 below which shows the ambient temperature after each simulation. Clearly it rises initially due to the primary effect of the human, before rising marginally again and converging at around 294.72°C (a rise of 1.72°C). All temperature inputs and outputs can be viewed in Appendix C.

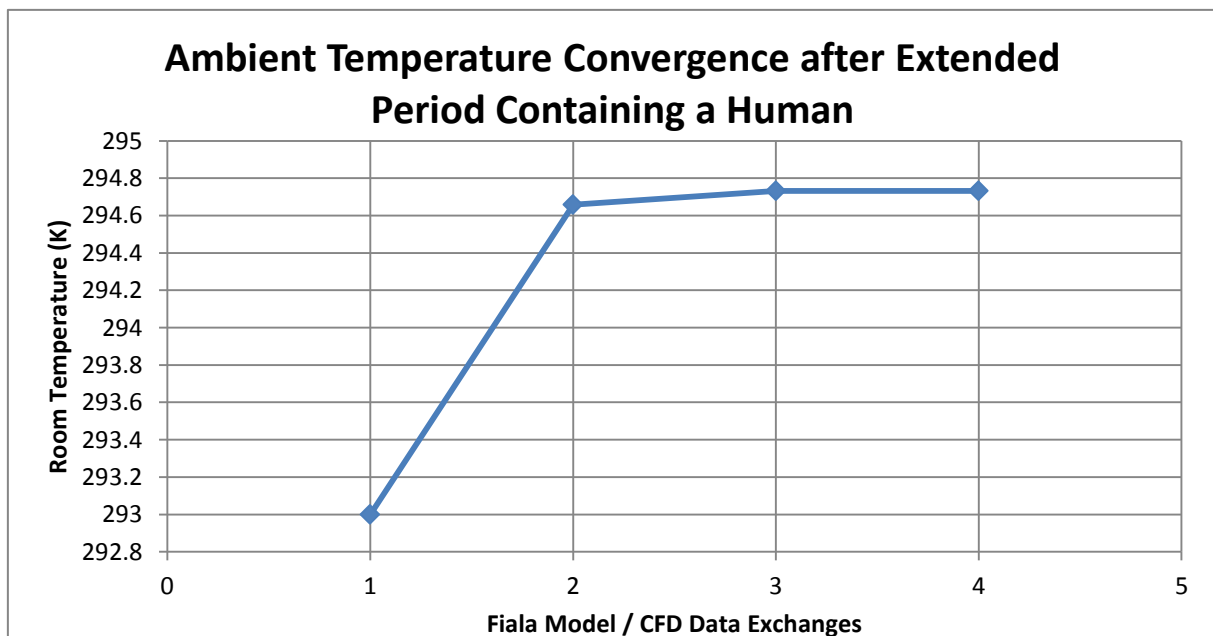


Figure 22 – Room Temperature Convergence

This converged value is the predicted average temperature value of the room due to human heat and natural convection after an extended period of time. The temperature contours can be seen in Figure 23. After convergence, a clear thermal plume can be seen, as air heats up from the skin surfaces, before drifting upwards due to buoyancy effects and out of the two outlet vents (as seen from the YZ plane). The Fiala model predicted the most heat around the head, shoulders and underarms as would be expected. Figure 24 shows velocity vectors in the Y direction across three planes in the domain. Clearly the flow accelerates above the shoulders due to buoyancy, whilst higher velocity air is also visible at the inlets as new air is forced back into the domain. These results agree with data shown by Cropper et al. in previous works [2]. Further visualisation for this case can be view in Appendix C.

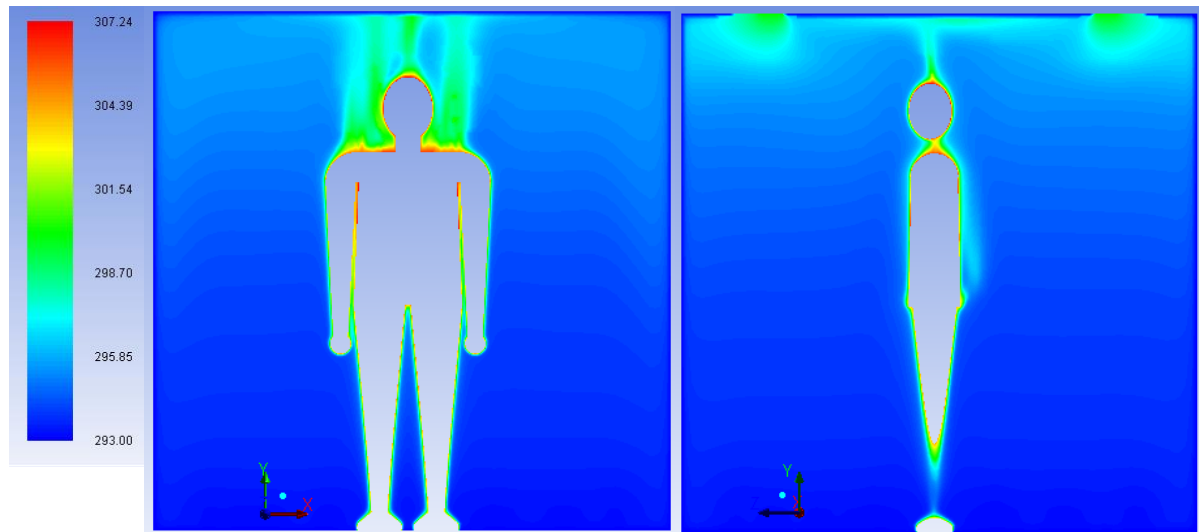


Figure 23 – Temperature Contours from XY and YZ Midplanes

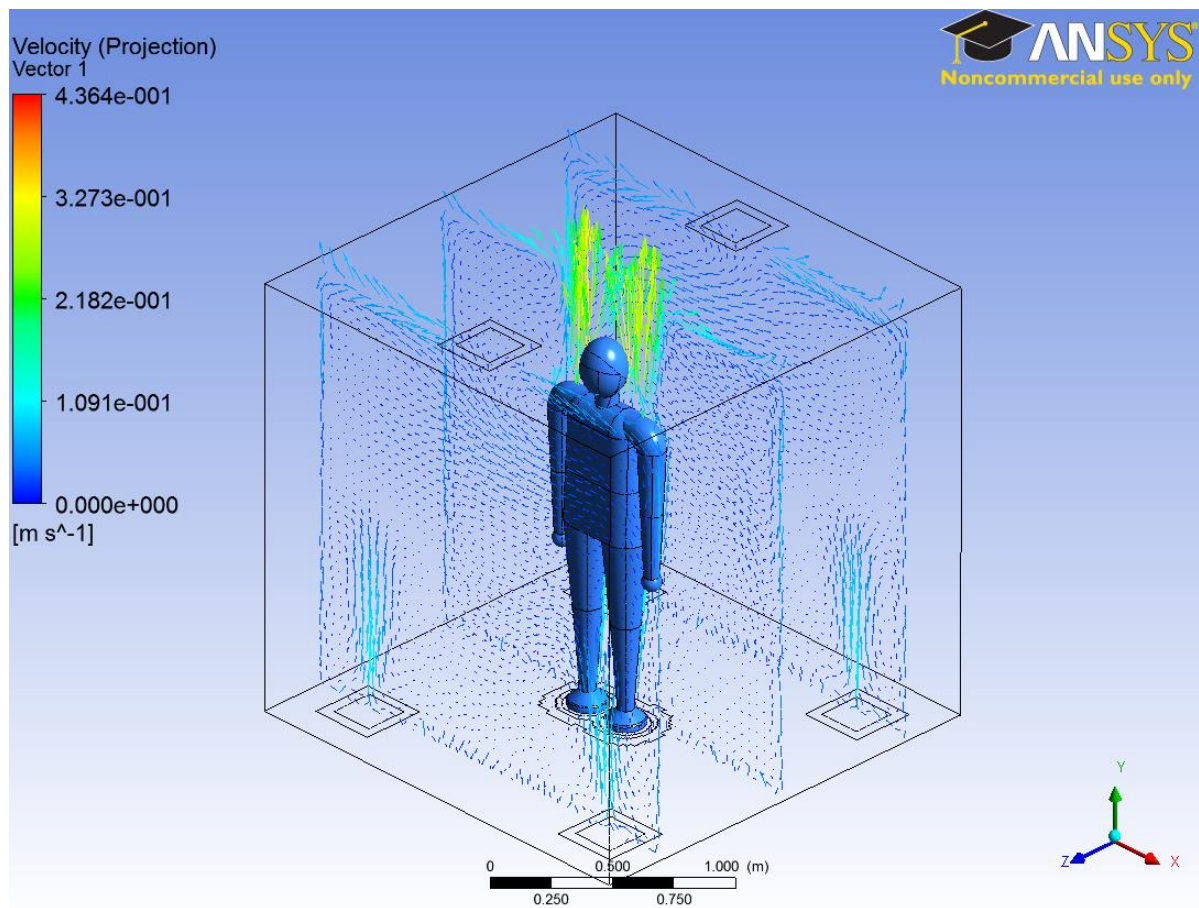


Figure 24 – Velocity Vectors in Y Direction in Natural Convection Domain

Temperature was plotted along two lines in the domain using the CFD-Post capabilities. Figure 25 shows the position of the lines in order to understand the temperature variance in Figure 26. The plot of the temperature variance just above head height describes the thermal plume effectively, where the temperature starts at 294K just beside the cold walls, before rising to 295.6K above the shoulders and rising further and peaking at 297.6K above the head, before mirroring the left hand side towards the right hand wall. This is expected with the head being the warmest part of the body, both in theory and according to the Fiala outputs. Of course the head is closer to the line than the shoulders, so the heat is less likely to have dispersed once it has reached it. The second line, placed just behind the body in order to obtain a full graph, shows a linear increase in temperature from the floor upwards. Again this is expected due to buoyancy effects and new cold air entering through the floor.

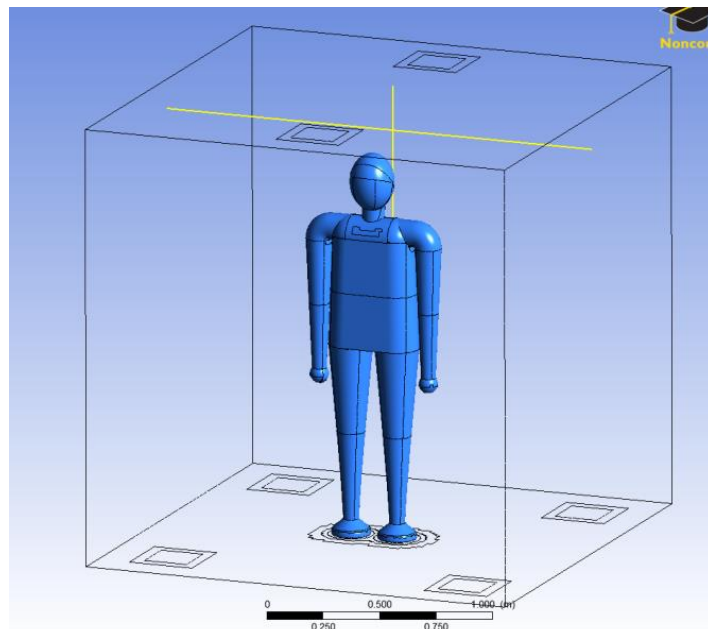


Figure 25 – Position of Sample Lines within the Domain

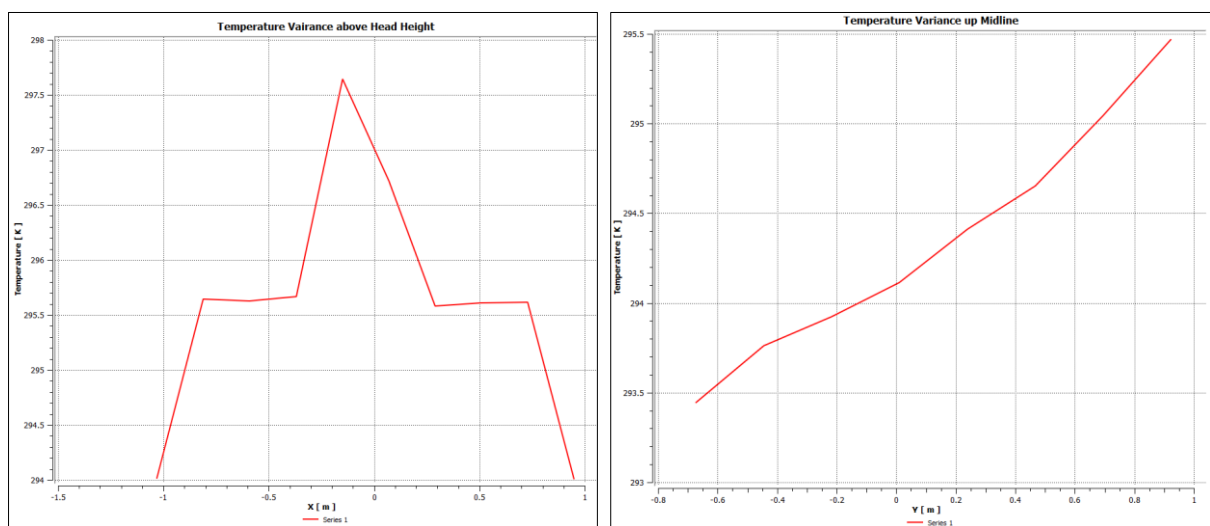


Figure 26 – Temperature Variance above the Head (Left) and Behind the Body (Right)

6.2. Human and Room 170 Integration

Similarly to the free convection problem, the temperature convergence was evident after a number of time steps (Figure 27). On this occasion, temperatures only rose by 0.25°C in total. As well as this, the converged temperature was much lower than that of the free convection. This is because the initial temperature reading achieved in the Room 170 was around 18.518°C due to the cold inlet air from the ceiling above the human. This initial condition was taken before the human had an effect on the room, allowing the Fiala model to be run with conditions that matched the initial CFD set up.

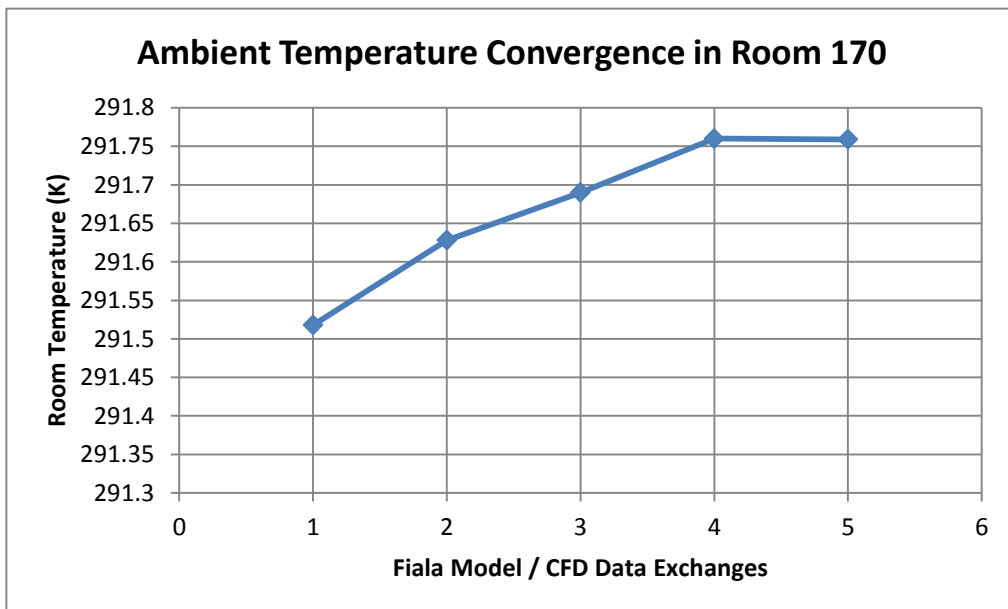


Figure 27 – Temperature Convergence in Room 170

It can be seen that convergence was achieved after 5 exchanges, and the average temperature (measured using the surface of revolution mentioned earlier) around the human converged at 291.76K (18.76°C). The difference in temperature is due to the air conditioning present in Room 170 compared to in the natural ventilation case. Figure 28 displays temperature contours around the human before and after the effect of its own heat. Air velocity was also present meaning heat would be carried away from the human due to forced convection, compared to the previous case. This velocity was taken into account when running the Fiala model, and was found using the same method as for temperature. With other heat sources present in the room, the model was more complex than the natural convection .In this case, the K-Epsilon turbulence model was chosen, as chosen by Locci due to its high performance with isotropic flows in complex geometries [38]. The Boussinesq approximation was again included in the model to simulate buoyancy effectively. The mesh was less dense than in the previous case due to its size, however refinements were still present around heat sources, inlets and outlets, making it accurate enough for residual convergence.

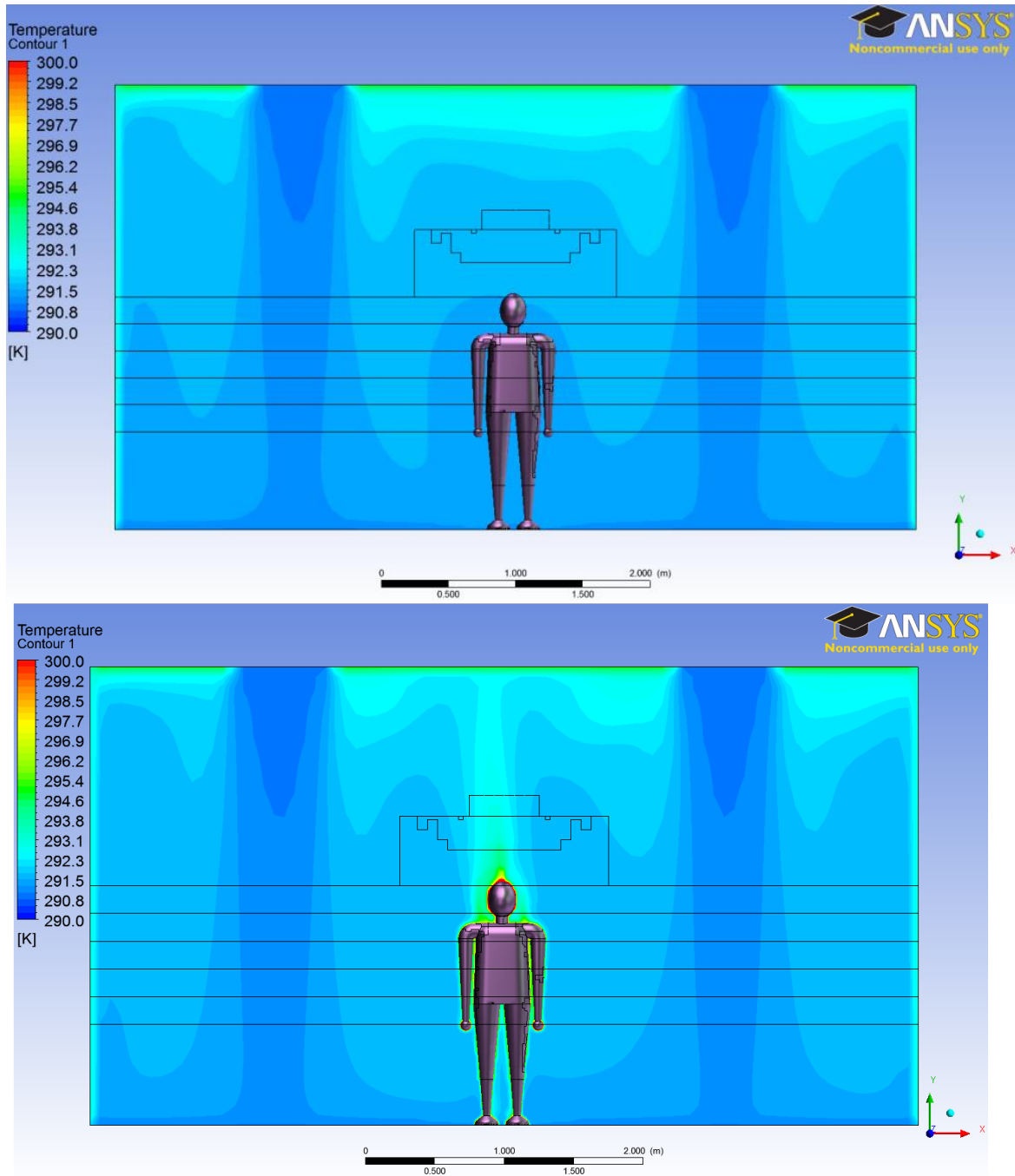


Figure 28 – Temperature Contours Before and After the Impact of the Human

The temperature contours above initially show warmer air at the top of the room. This is due to the effect of other heat sources in the room such as the computer and projector. The darker blue indicates where the colder inlet air is blown downwards into the room, before dispersing and diffusing outwards. The contours after the human had an impact show a definite plume above the head of the body, where buoyant air is rising to the top. This is as expected, and as mentioned earlier the overall change in temperature is less noticeable due to the other heat sources and air conditioning affecting the room already.

7. Discussion and Comparison of Results

The results displayed in section 6 outlined how humans have an effect on the local environment, and how after enough time the surroundings stabilise to an average temperature, as does the human body.

Unfortunately due to time constraints, the sensor group were unable to produce sensors in time to draw comparisons with experimental data. Nonetheless, it was possible to compare some results with previous works and with heat transfer theory. Cropper et al. in previous works carried out a similar simulation for natural convection, only with a clothed model with more detail. He calculated convection coefficients, which could be compared with the convection coefficients generated in this work by the Fiala model. Due to the large number of faces, the generated coefficients were averaged for each body part. These can be seen in Figure 29 for both cases in this work as well as Cropper et al.'s previous work.

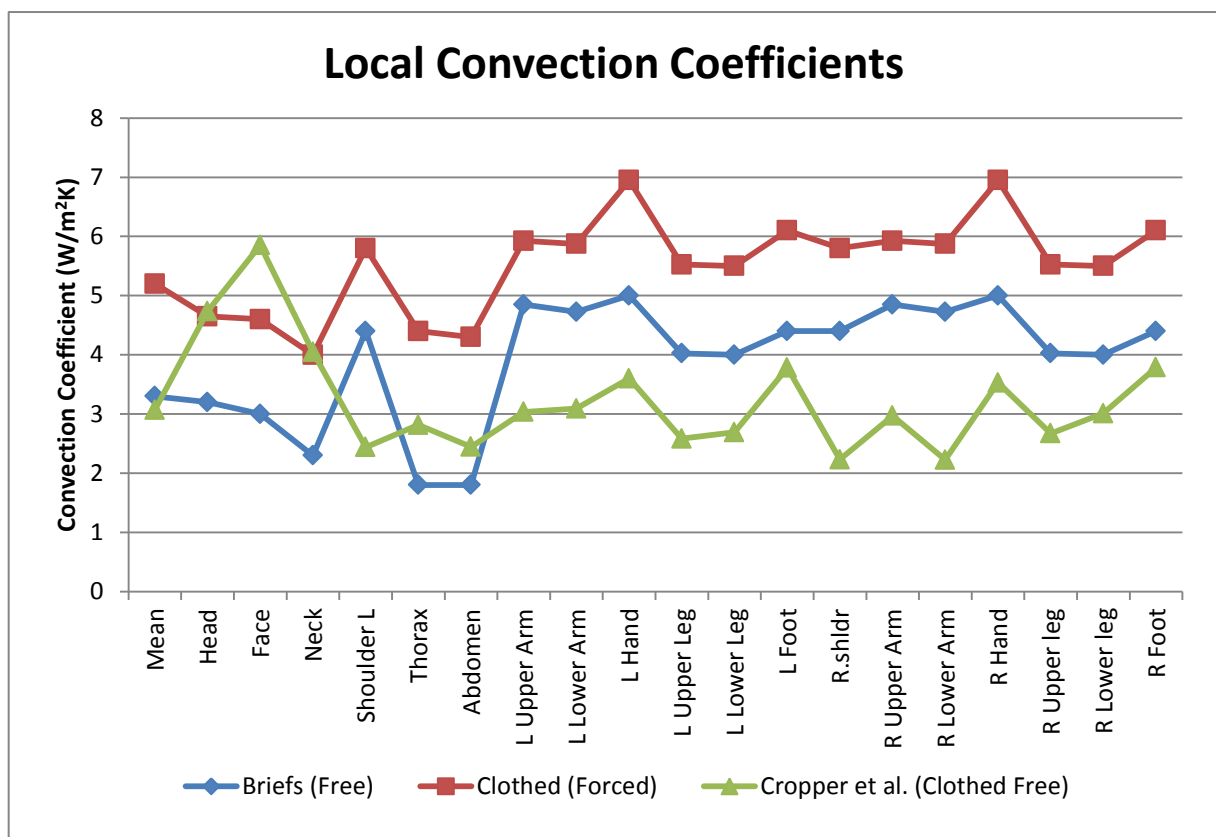


Figure 29 – Convection Coefficients for Both Cases Compared with Work by Cropper et al.

Output results for convection coefficients were found to correlate well with those found by Cropper et al. when he used the Fiala model for a clothed male in a naturally ventilated space. Whilst the data values do not exactly match up, they all show similar trends, with low coefficients at the thorax and abdomen, and slightly higher coefficients at the lower arms and hands. The differences are due to the varying operating conditions. As only skin convective coefficients were available from the Fiala model, the clothed model shows the highest results. This is because the skin is heated up due to the insulation, and convecting more heat as a result. The human in briefs, shows the same pattern but with lower values, as the body was not insulated, the skin temperatures were slightly lower, as were the convection coefficients.

The results obtained by Cropper et al. were calculated in the CFD part of the work, based on the surface areas of their own geometry. These coefficients were also obtained from the clothing surface, which would be cooler than the skin, hence the lower values. Looking at the mean values from Cropper et al. and the natural convection case (male wearing briefs) the values differ only slightly, with the Cropper et al. mean lower by 0.23 W/m²K, due to the reduced heat from clothing.

Using equation 3 in the theory section, a value of 83W was obtained for the overall convective heat loss of the human. The mean convective heat loss coefficient was obtained from the Fiala model, which it predicted to be 3.3 W/m²K. The ambient temperature was 20°C and the average skin temperature (taken from the Fiala model again) was 33.6°C. The body surface area was taken as 1.85m². Comparing this to the convective heat loss predicted by the Fiala model of 74W, there is a difference of around 11%. This is perhaps down to a number of different parameters used in the complicated Fiala model, as well as the difference in temperatures over time. It is also likely to be affected by the averages taken in the calculations. Each temperature represents an area, some of which are larger than others. Therefore by averaging them, the resultant heat loss may be inaccurate.

Of course, the exact values obtained are unlikely to be the same as temperatures recorded in a room of the same dimensions. This is due to how the case is set up, with initial conditions assumed before the CFD can be carried out. In an ideal world, sensors would have taken values for walls, and air in the centre of the room, which would have been used as Fiala inputs. With a level of consistency, a direct comparison could have been made, but this is always a challenge to achieve. The human needs to adjust as well, for example if values were taken just after the human had come from a cold environment or a very hot environment, the initial conditions would be different. The Fiala model is run in a way that convergence is achieved, so initial conditions for the model are not a damaging factor. This is not possible experimentally however, making validation more complicated.

A number of other factors would affect the simulation in real life, such as hair on the head, which is neglected by the Fiala model (the back of the head is always the hottest, where in actual fact the hair temperature would be reduced due to its insulating properties). Humidity is another issue that is not tackled in this project. Whilst measuring humidity experimentally is not too challenging, simulating it in CFD can be more difficult. VOF (volume of fluid) methods are required for this, meaning the program simulates the movement of both air and water at a pre-defined fraction. With the moisture being generated on the skin surface, this process would be highly challenging, and was beyond the scope of the project.

The work looked at in the results focuses only on one human. Of course, with more than one human, the effects on the room are likely to be much more significant, with more heat being generated, and therefore the humans heating up more as a result. This could be modelled in a similar way, and would not be too difficult to implement. Although the Fiala model was not used, Smith briefly looked at modelling multiple basic humans in Room 170 [17]. The results in this work also look only at convection, without touching on radiation. The reason for this is that radiation models are complex to set up, with various different methods and view factors

being taken into account as well. With the relatively low temperature of the human body, radiation was considered to be of small importance. It was also less important as it only noticeably heats surfaces directly, and as this work was looking at the immediate environment, convection was much more important.

8. Sustainability

It is important to assess all engineering projects on sustainability as well as results. This is because in the modern industry, any work can have a knock on effect to the environment, society and economy. Therefore, complying with the modern guidelines is paramount in order to justify new developments and deem them sustainable in the long term.

8.1. Society

The intentions of the work carried out in this project look at improving the built environment for its occupants in the modern times of rising temperatures. Although this aim is not directly worked on, the models used in the work can be used again with varying operating/boundary conditions in a way to test out differing environments in various settings. The work is therefore deemed to have a positive effect on society, as it looks at improving working/living conditions to comply with human comfort.

8.2. Environmental

The project as a whole is more focused on the environmental factors than any other. Whilst the work does not necessarily prevent or reduce global warming, it does look at a method to mitigate the effects of rising temperatures. The study on how humans affect the local environment allows architects and engineers to incorporate this model into building design. The newer efficient designs that take these factors into account are less likely to use excess energy to create cooling systems. Instead, natural ventilation can be utilised and can be optimised to work effectively based on the number of occupants in a room at any time. In the long term, this would of course reduce the use of fossil fuels to produce energy for cooling systems for improving thermal comfort. For these reasons, the project is considered environmentally sustainable. However, one factor to counter this is the use of computational modelling. On a large scale, CFD is very expensive and consumes a lot of energy. The question is whether the energy is offset by that saved from the outcomes, potentially reducing the sustainability of the work.

8.3. Economy

Finally, it is important to assess the economic impact of the project. As mentioned in the environmental section, the key financial challenge arising from this work is the cost of the computational methods. In order to take this work to an industrial level, highly expensive machines and technology would be required. A benefit however would be the reduced cost of air conditioning in future built environments, improving the economic sustainability. The cost of CFD can be less expensive than sensors and experimental equipment making it more economically sustainable.

9. Project Management

9.1. Group Work

Working in a group towards a collective set of aims required each member to work in a disciplined manner to achieve their individual tasks. In order to complete all of the tasks assigned to this work, a personal Gantt chart was produced with deadlines for completion. This can be viewed in Appendix A, and was edited slightly from the chart in the I1 report earlier in the project. This was to incorporate the updated objectives. Each deadline was met efficiently. The only change in the plan occurred when the decision was made to work with the initial geometry generated instead of spending time making more complex figures. This decision was made to save time in the long run, as the initial design was considered adequate for the simulations carried out. This allowed more time to carry out the more complex tasks of coupling together the two models and running them effectively and efficiently. The use of this chart allowed me to work to deadlines and complete the objectives outlined in the introduction. Another aspect of management that was tackled well by the group was the weekly meetings to discuss progress. These were also attended by Dr Gavin Tabor, research fellow Dr Matt Eames and PhD researcher Ed Shorthouse. As well as these, the group also held separate meetings later in the week. The project was managed on the whole very well, with different roles allocated early on, and communication well maintained throughout. The only drawback was the lack of experimental data produced by the electronics group. This could have been managed slightly better in order to ensure data was recorded in time.

9.2. Budgeting

The group was entitled to £80 budget per head. As most of this was to be spent on electronic parts for the building of sensors, a relatively small amount was spent on the human aspect. In total two items were bought; Logitech C525 HD Webcam £35.29 and a Red Laser Line, 5mW, Battery-Operated, 90° CLASS 1 - £24 + VAT. These came to just under £60, remaining well inside the combined £160 budget of Tompsett and myself. Pamatmat was assigned as the group treasurer at the start of the project and kept a record of any money spent, ensuring the budget was kept to.

9.3. Health and Safety

The only procedure that required any health and safety input in this project was the use of a line laser in the human scanning. With the initial plan to scan a human, it was vitally important that the laser was eye-safe in the class 1 laser safety category. This was in fact carried out when the laser was purchased, however it was not required in the end as it was discovered that scanning a human would be impractical and challenging beyond the scope of the project.

10. Conclusion

The individual aim of this project from the outset was to generate a CFD model that incorporated human thermal comfort in order to accurately model the effect of a human on the local environment. The project first looked at producing a suitable geometry to run simulations on, before investigating the modelling of natural and forced convection in ANSYS Fluent. This was followed by applying the methods to the geometry generated, before looking in detail at the Fiala human comfort model and eventually coupling both models together. This was carried out first for a simple natural convection case, before using it to model the human in the chosen room Harrison 170.

On the whole the project proved successful and showed that coupling the human responses and the environment responses displayed a noticeable difference in the surroundings. With natural convection, the human caused an overall temperature rise of 1.72°C whilst the ventilated room showed a rise of 0.25°C after the convergence of both models.

Having achieved all of the aims set out, there were a number of challenges that were overcome along the way. One of the key challenges was setting up the CFD simulation to run effectively, producing convergence in the mesh and generating accurate data as a result. For the natural convection case, this challenge was overcome by running a mesh refinement study, increasing detail at the surfaces of the human, the walls and the mesh. This is because a large part of convection occurs at the boundary layer between the surface and where the flow has a velocity. With more time and available computing power, a mesh of several million cells would be set up to ensure an entirely accurate set of data, with no mesh originating issues. To obtain a mesh that was good quality, the relatively recent addition of cut cell meshing to Fluent was utilised. Generating predominantly hexahedral cells, with wedges and tetrahedral cells added at curved surfaces, the average cell quality was as high as 98% in the densest mesh.

One of the aims of the project that was not achieved was the scanning of a member of the group for an accurate human model. The reason for this was the cost of the equipment that would be required. Also, a testing rig would have been required to set up the group member to be consistently still during the scanning. Therefore, with the time scale of the project and financial restraints the decision was made to use the geometry generated on Solidworks.

Without a doubt, the largest obstacle that was targeted at the start of the project was incorporating the human comfort model into the CFD simulations. This was achieved, albeit manually, and produced results that correlate with what is expected as well as previous literature. As previous works achieved this by coding scripts which computationally tell each model when and where to feed results into the other, the task would always be highly challenging. As neither Tompsett nor I have any experience with coding, the decision was made to manually couple the two. This was more time consuming as it meant sorting data from text files in Excel and manually entering the results as boundary conditions into Fluent. Whilst this made the process more time consuming, it also saved time in the long run, as learning how to code the process would have taken a large amount of time and may not have been accomplished to a satisfactory level, leaving the project incomplete. Learning how to use

the Fiala model was not as challenging as first thought but it still required time and patience to understand before incorporating it into the CFD model, which required modification of the geometry as described in the methodology.

Overall, the project generated a model that couples CFD with human comfort to describe how the local environment is affected by the human. With the overall project looking at how climate change affects the human and built environment, the work carried out in this project could easily be used again with modified boundary conditions to model how the built environment changes with weather conditions.

11. Future Work

Whilst this project achieved the aims that were set, there are a number of areas which could be improved with further work.

The CFD work in this project focused on convection; free and forced, but did not look at the effects of radiation and humidity. This was due to the complexity of the CFD models that would be required, and the financial and computational restraints of the project. However, with access to both of these resources, radiation and humidity could be modelled in Fluent to give a more complete overview of the environmental changes. Another change that could be implemented is the addition of further bodies. The work in this project focused on one body and obtaining accurate data for that figure, however with the model clearly defined, expanding the case to a number of standing humans would not be excessively challenging. This could still incorporate the human comfort model, although more accurate averaging systems would be required to measure the ambient conditions. To more realistically model a lecture theatre or classroom, a number of sitting geometries could also be generated, and a lecture could be modelled and compared to data over a set period of time. With a lot more time, a full set of data could be recorded for humidity, temperature and air velocities and compared to CFD predictions for validation. The option to expand up to larger buildings like train stations or vehicles such as trains and planes is also an avenue worth exploring. The processes of the research would be the same, only with different geometries and boundary conditions.

Whilst it would be very challenging, a long term objective would be to produce a model that incorporates moving humans. This would require much more detailed CFD work, as a moving mesh would be needed. As well as this, the human comfort model looks entirely at an average male. If a model was available for women and children in the future, this would certainly be applicable and would offer a more accurate representation of the human population. Some other factors not included in the human comfort model are perhaps more random occurrences, such as high stress levels or illness causing temperature rises. Of course this is difficult to model, but could potentially be incorporated in the long term.

With the knowledge of a computer programmer and a larger time scale, a process similar to that of Cropper et al. could be utilised to program the coupling process. This would allow simulations to run far quicker, as well as allowing cut off values to select when to allow data

exchanges and when the solution has converged. With this addition, simulations on a much larger scale could be left to run on a super computer without tedious manual data exchanges.

A potentially very important development in this field is to carry out the methods described in this report but in a transient case, coupling results from the Fiala model and the CFD case after every time step, to gain a realistic understanding of the change with time. This would certainly require coding to carry out and further research. Finally, to fully validate the CFD being used, the turbulence models and solution methods would need to be validated using comparison studies of all the suitable models and deduce the most appropriate.

References

- [1] IUCN, “Facts and Figure on Climate Change,” 26 April 2010. [Online]. Available: http://www.iucn.org/about/union/secretariat/offices/oceania/oceania_resources_and_publications/?9711/Facts-and-figures-on-Climate-Change.
- [2] P. Cropper and T. Yang et al, “Coupling a model of human thermoregulation with computational fluid dynamics for predicting human environmental interaction,” Loughborough University, 2009.
- [3] A. P. Gagge, P. Stolwijk and J. Hardy, “Comfort and Thermal Sensations and Associated Physiological Responses at Various Ambient Temperatures,” *Environmental Research*, vol. 1, pp. 1-20, 1967.
- [4] G. Fu, “A Transient 3-D Mathematical Thermal Model for the Clothed Human,” 1995.
- [5] R. Holopainen, “A Human Thermal Model for Improved Thermal Comfort,” VTT technical Research Centre of Finland, Aalto, 2012.
- [6] M. Fountain and C. Huizenga, “A Thermal Sensation Prediction Tool for Use by the Profession,” *ASHRAE*, 1997.
- [7] Jones and W. Byron, “Capabilities and Limitations of Thermal Models,” Kansas State University, 1998.
- [8] B. Jones and Y. Ogawa, “Transient Interaction Beteen the Human Body and the Thermal Environment,” *Ashrae Transactions*, vol. 98, no. 1, 1992.
- [9] Y. Ozeki and S. Tanabe et al., “Angle factors between human body and rectangular planes calculated by a numerical model,” *Ashrae Transactions*, 2000.
- [10] S. Tanabe and K. Kobayashi et al, “Evaluaton of thermal comfort using combined multi-node thermoregulation (65MN) and radiaton models and computational fluid dynamics(CFD),” *Energy and Buildings*, vol. 34, no. 2002, pp. 637-646, 2002.
- [11] “IESD-Fiala Model,” [Online]. Available: http://www.iesd.dmu.ac.uk/~yzhang/wiki/doku.php?id=software:model:iesd_fiala:introduction.
- [12] D. Fiala, K. Lomas and Stohrer, “Computer prediction of human thermoregulatory and temperature responses to a wide range of environmenal conditions,” *Int J Biometeorol*, vol. 45, pp. 143-159, 2001.

- [13] S. Murakami, K. S and J. Zeng, "Combined simulation of airflow, radiation and moisture transport for heat release from a human body," *Building and Environment*, vol. 35, pp. 489-500, 2000.
- [14] P. Cropper et al, "Simulating the effect of complex indoor environmental conditions on human thermal comfort," Glasgow, 2009.
- [15] M. Hadjukiewicz et al, "Formal calibration methodology for a CFD model of a naturally ventilated room," in *Proceedings of Building Simulation*, Sydney, 2011.
- [16] M. Loomans, "The Measurement and Simulation of Indoor Air Flow," *Dutch Organisation for Scientific Research*, 1998.
- [17] A. Smith, "Using CFD as a Tool for Designing the Built Environment," University of Exeter, 2013.
- [18] N. P. Gao and J. L. Niu, "CFD Study of the Thermal Environment around a Human Body: A Review," *Indoor and Built Environment*, vol. 14, no. 1, pp. 5-16, 2005.
- [19] L. Davidson and P. V. Nielsen, "Calculation of the two-dimensional airflow in facial regions and nasal cavity using an unstructured finite volume solver," Department of Building Technology and Structure Engineering, Aalborg University, Denmark, 1995.
- [20] T. French, "Modelling the Response of Humans to Varying Conditions in a Built Environment, and the Effect of Humans on the Built Environment: Review and Future Work," University of Exeter, 2012.
- [21] S. K. S. Choi, "Turbulence modelling of natural convection in enclosures: A review," *Mechanical Science and Technology*, vol. 26, no. 1, pp. 283-297, 2011.
- [22] M. S. Cramer, "Foundations of Fluid Mechanics; Navier-Stokes Equations," Cambridge University Press, 2004. [Online]. Available: <http://www.navier-stokes.net/nsdef.htm>.
- [23] SharcNet, "The K-Epsilon Model," 2010. [Online]. Available: https://www.sharcnet.ca/Software/Fluent13/help/cfx_mod/i1345899.html.
- [24] D. C. Wilcox, "Turbulence Modeling for CFD," DCW Industries, La Canada, California, 1998.
- [25] D. A. Gerasimov, "Modelling Turbulent Flows with FLUENT," 2006. [Online]. Available: http://www.ae.metu.edu.tr/seminar/Turbulence_Seminar/Modelling_turbulent_flows_with_FLUENT.pdf.
- [26] ANSYS, "Shear-Stress Transport (SST) k-omega Model," 23 January 2009. [Online].

- Available: <https://www.sharcnet.ca/Software/Fluent12/html/th/node67.htm#13998>.
- [27] D. S. Ghorai, “The Boussinesq Approximation,” 16th January 2003. [Online]. Available: <http://home.iitk.ac.in/~sghorai/NOTES/benard/node3.html>.
- [28] ANSYS FLUENT, “Natural Convection and Buoyancy-Driven Flows,” 20th September 2006. [Online]. Available: <http://cdlab2.fluid.tuwien.ac.at/LEHRE/TURB/Fluent.Inc/fluent6.3.26/help/html/ug/node572.htm>.
- [29] D. Fiala et al, “UTCI-Fiala multi-node model of human heat transfer and temperature regulation,” *International J. Biometeorol*, vol. 56, pp. 429-441, 2012.
- [30] J. Chen et al, “3D shape modelling using a self-developed hand-held 3D laser scanner and an efficient HT-ICP point cloud registration algorithm,” *Optics and Laser Technology*, vol. 45, pp. 414-423, 2013.
- [31] K. Franke et al, “Low-Cost Laser range scanner and fast surface registration approach,” *Springer Berling*, pp. 718-728, 2006.
- [32] G. Locci, “CFD Modelling of Lecture Room and Integration of a Human Body,” University of Exeter, 2013.
- [33] J. Bunting, “Review of the Lumped Parameter Model and Study of its Application to a Room in the Engineering Building,” University of Exeter, 2013.
- [34] K. Pamatmat, “Research and Instrumentation of Key Environmental Sensors for CFD Validation of a Built Environment,” University of Exeter, 2013.
- [35] M. Dalladay-Simpson, “Research, Design and Implementation of a Custom Data Logging Network for a Small Lecture Theatre,” University of Exeter, 2013.
- [36] P. Tompsett, “CFD Modelling of a Buoyancy-Driven Flow around a Simplified Human Form in a Naturally Ventilated Room,” University of Exeter, 2013.
- [37] D. D. Fiala, “Dynamic Simulation of Human Heat Transfer and Thermal Comfort; The IESD-FIALA Model User Guide,” De Montford University, 2008.
- [38] B. Tartinville and C. Hirsch, “Reynold-Averaged Navier Stokes Modelling for Industrial Applications,” Belgium, 2009.

Appendix A

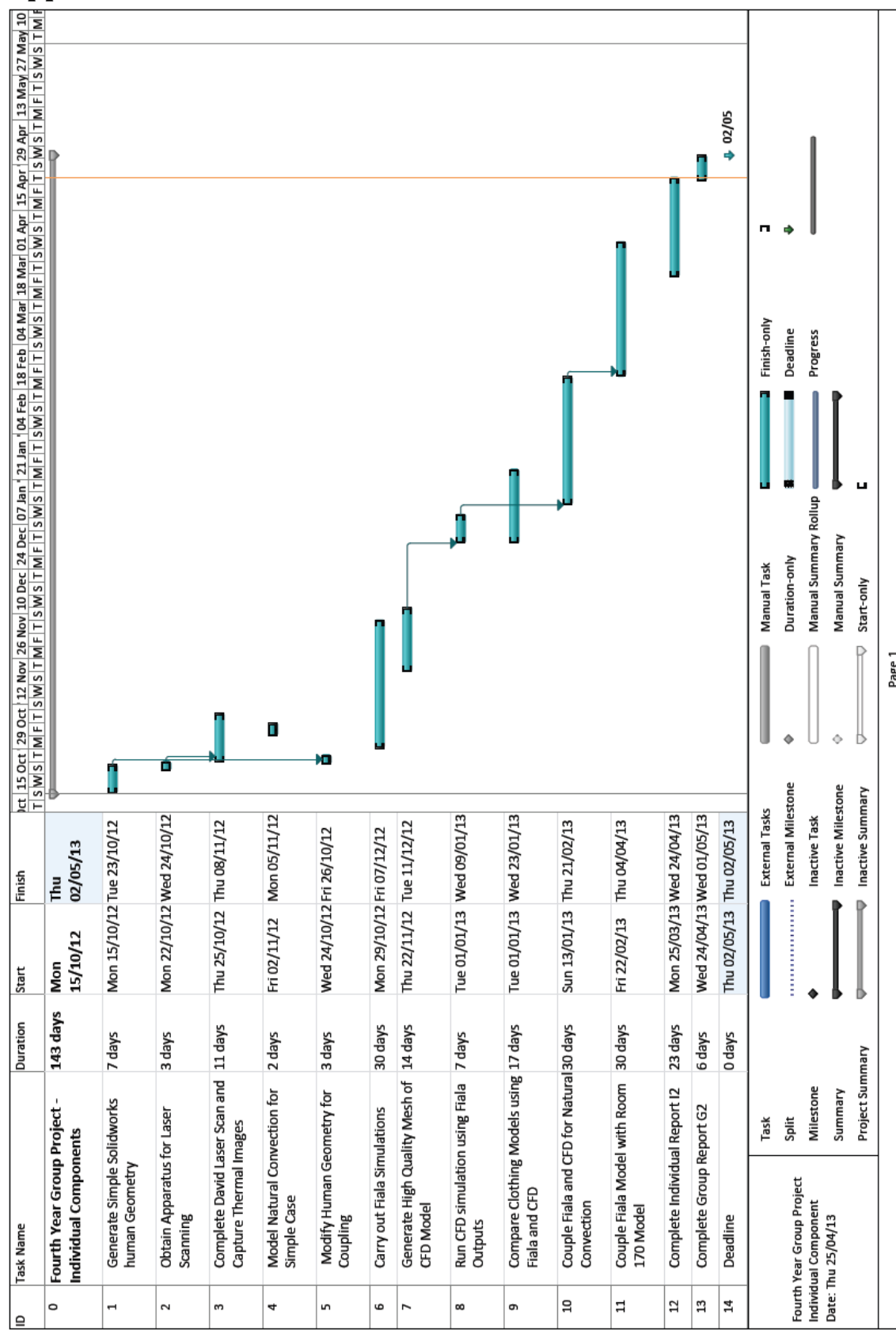


Figure 30 – Management Gantt chart

Appendix B

Table 4 shows details of the mesh convergence study carried out in preparation for running the free convection coupling process. Figure 31 shows the mesh detail around the human with a high level of refinement accounting for boundary layer flow.

Table 4 – Details of Mesh Convergence Study

	Mesh 1	Mesh 2	Mesh 3	Mesh 4	Mesh 5
Elements	380,710	665592	960654	2202569	2766469
Nodes	423632	728411	1077856	2482111	3058020
Body Sizing (m)	0.01	0.008	0.006	0.004	0.003
Vents Sizing (m)	0.01	0.01	0.01	0.009	0.008
Walls Sizing (m)	0.05	0.04	0.03	0.03	0.02
Max Velocity (m/s)	0.2	0.362	0.36778	0.399	0.40693
max Dynamic Pressure (Pa)	0.01515	0.08155	0.0853	0.09605	0.099969
Total Force Y	2.029908	2.044	1.886444	1.853	1.907496
Mas Flow Rate	-6.63E-05	-0.00012	4.68E-06	4.84E-05	4.66E-06
Total Heat Transfer Rate	23.24569	33.986	23.71399	23.1125	20.65725

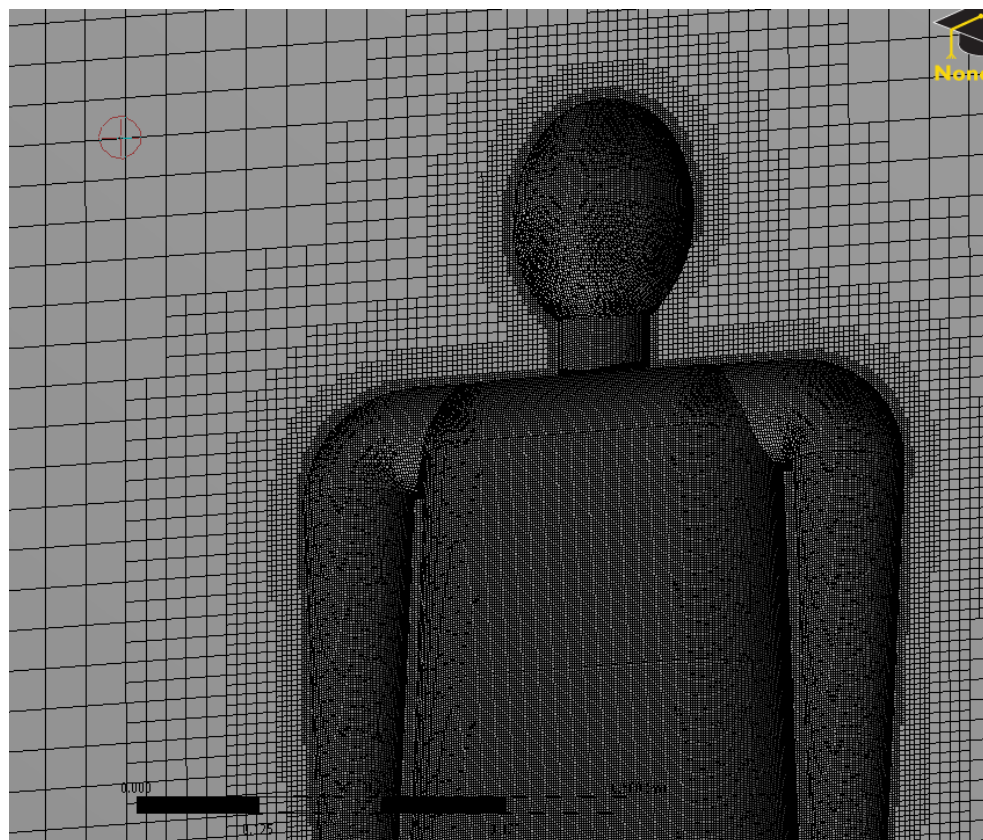


Figure 31 – Mesh Refinement at Human Surface with Extra Detail at Boundary Layer

Appendix C

The following tables outline the inputs and outputs obtained from the coupling process. The inputs were used to run the Fiala model and were incorporated into Boundary Condition Files. The outputs are the surface temperatures generated by the Fiala model after the body stabilised. In Table 5, the outputs were averaged over larger body parts, hence fewer faces. Table 6 on the other hand contains output data for all 59 faces of the body.

Table 5 – Fiala Outputs for Coupling with Room 170

	Fiala Run 1	Fiala Run 2	Fiala Run 3	Fiala Run 4	Fiala Run 5
Inputs					
Ta	291.518	291.628	291.69	291.76	291.759
Tw	293	293	293	293	293
Va	0.14	0.14	0.14	0.14	0.14
Hr	0.3	0.3	0.3	0.3	0.3
Activ	2	2	2	2	2
Outputs					
head	306.265	306.275	306.285	306.29	
face	305.33	305.39	305.41	305.43	
neck	299.9775	300.0133333	300.03	300.055	
shldr	297.13	297.18	297.2	297.23	
front	296.565	296.61	296.63	296.655	
back	296.545	296.585	295.5	296.635	
side	297.255	297.31	297.33	297.36	
arm	295.11375	295.17125	295.20375	295.23875	
hand	303.665	303.73	303.765	303.81	
leg	295.525	295.57625	295.6075	295.6375	
foot	298.49	298.545	298.57	298.605	

Table 6 – Inputs and Outputs for Fiala Free Convection Coupling

		Fiala Run 1	Fiala Run 2	Fiala Run 3	Fiala Run 4
Inputs					
Ta (K)		293	294.6586	294.7328	294.7324
Tw (K)		293	293	293	293
Va (m/s)		0	0	0	0
Hr (%)		0.3	0.3	0.3	0.3
Activ (MET)		2	2	2	2
Outputs (K)					
head	ant	306.56	579.56	306.7	
	pst	306.98	579.98	307.1	
	ant	302.68	575.68	303.5	
face	ext_l	302.59	575.59	303.41	
	ant	305.36	578.36	305.69	
	pst	305.08	578.08	305.42	
neck	ext_l	305.23	578.23	305.56	
shldr	left	304.87	577.87	305.06	
	ant	306.05	579.05	306.08	
Thorax	pst	305.99	578.99	306.02	
	l.inf	307.25	580.25	307.24	
	ant	303.02	576.02	303.14	

Abdomen	pst	303.03	576.03	303.14	
	l.inf	303.69	576.69	303.79	
	ant	302.5	575.5	302.82	
Upper Arm	pst	302.13	575.13	302.45	
	inf	303.51	576.51	303.87	
	ext	302.02	575.02	302.33	
	ant	301.68	574.68	302.01	
Lower Arm	pst	301.52	574.52	301.84	
	inf	302.47	575.47	302.82	
	ext	301.46	574.46	301.78	
Hand	hbk	302.84	575.84	303.33	
	plm	303.86	576.86	304.37	
	ant	303.58	576.58	303.8	
Upper Leg	pst	303.44	576.44	303.66	
	inf	304.61	577.61	304.84	
	ext	303.58	576.58	303.79	
	ant	303.4	576.4	303.6	
Lower Leg	pst	303.38	576.38	303.58	
	inf	303.87	576.87	304.08	
	ext	303.29	576.29	303.49	
Foot	inst	302.45	575.45	302.82	
	sole	302.38	575.38	302.74	

Figure 32 shows temperature contours on the human surfaces after having the Fiala outputs applied as boundary conditions. Clearly the back of the head and forehead are the warmest, with hot spots also located under the arms and legs. This explains why the thermal plume is more evident over the head and shoulders.

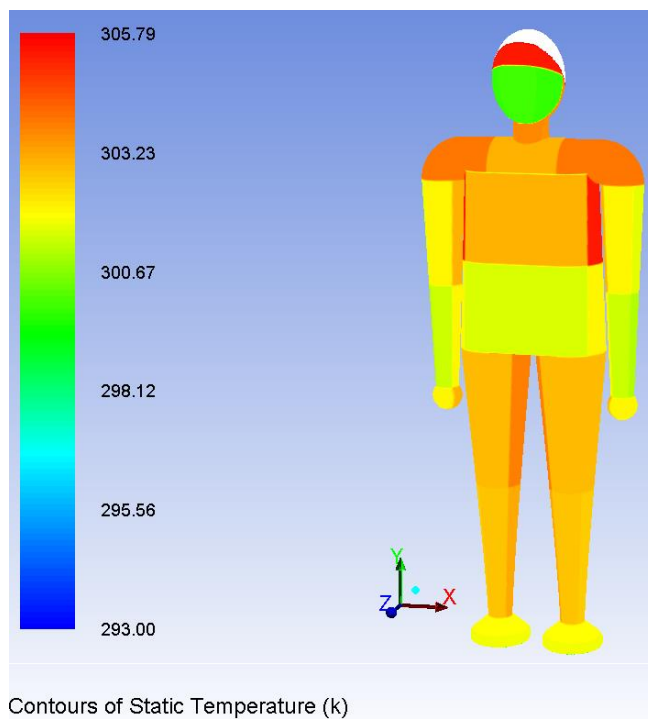


Figure 32 – Contours on Human Surfaces showing Fiala Output Temperatures

Figure 33 shows a volume rendering of temperature in the free convection, displaying clearly the rise in temperature above the human and the air leaving through the vents. Figure 34 shows a volume rendering of velocity in the control volume, clearly displaying an increase around the human as the air rises, as well as an increase as air is forced back into the domain through the inlet vents.

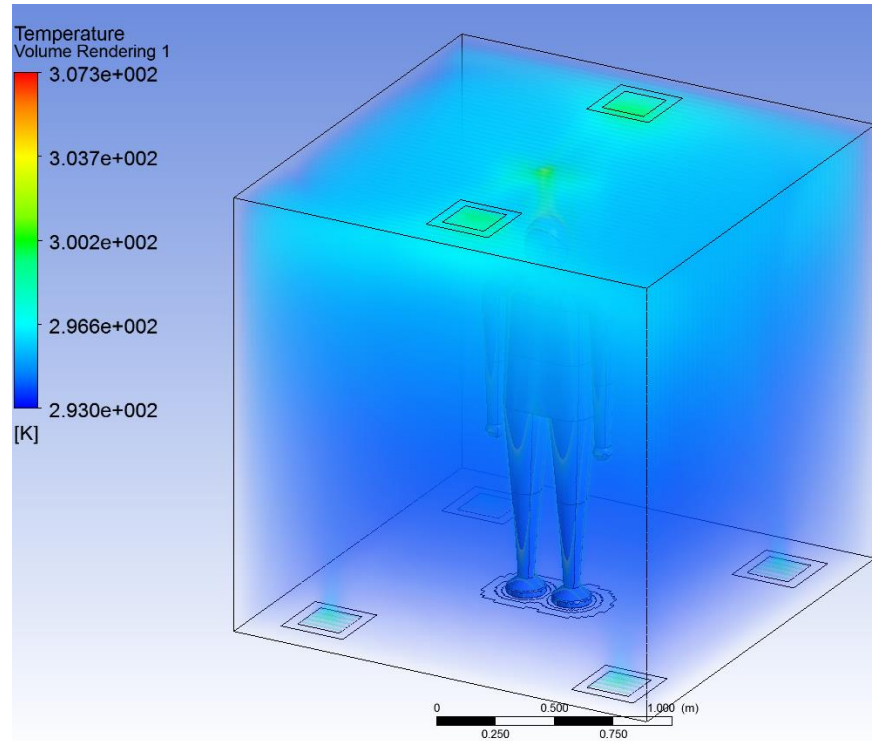


Figure 33 – Volume Rendering of Temperature for Free Convection Case

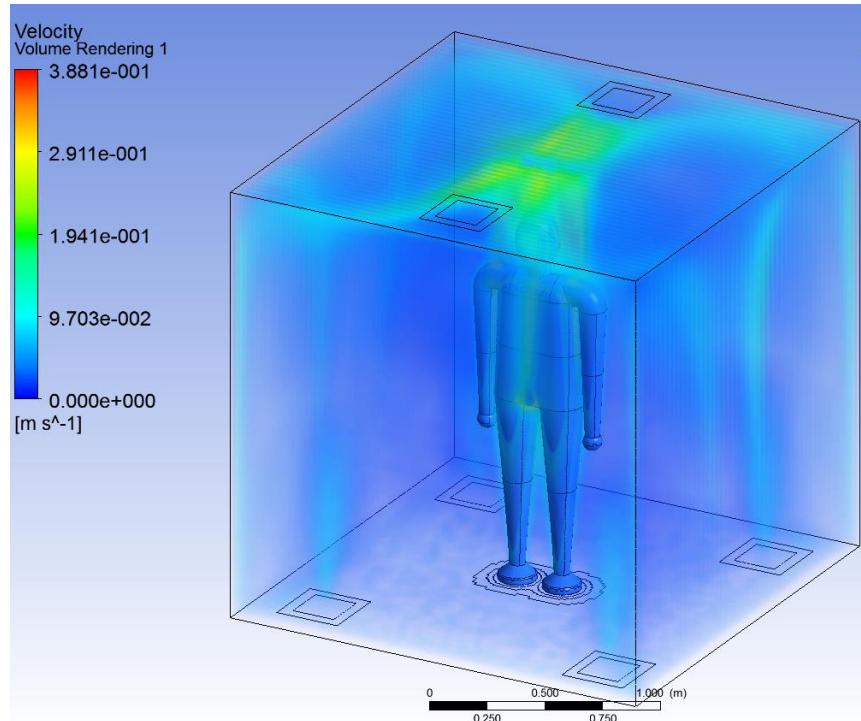


Figure 34 – Volume Rendering of Velocity for Free Convection Case

Appendix D

Figure 35 shows the dimensions of the test bed Room 170, drawn by the room group. Figure 36 shows the 3D model of the room containing the human geometry in preparation for coupling with the thermal comfort model.

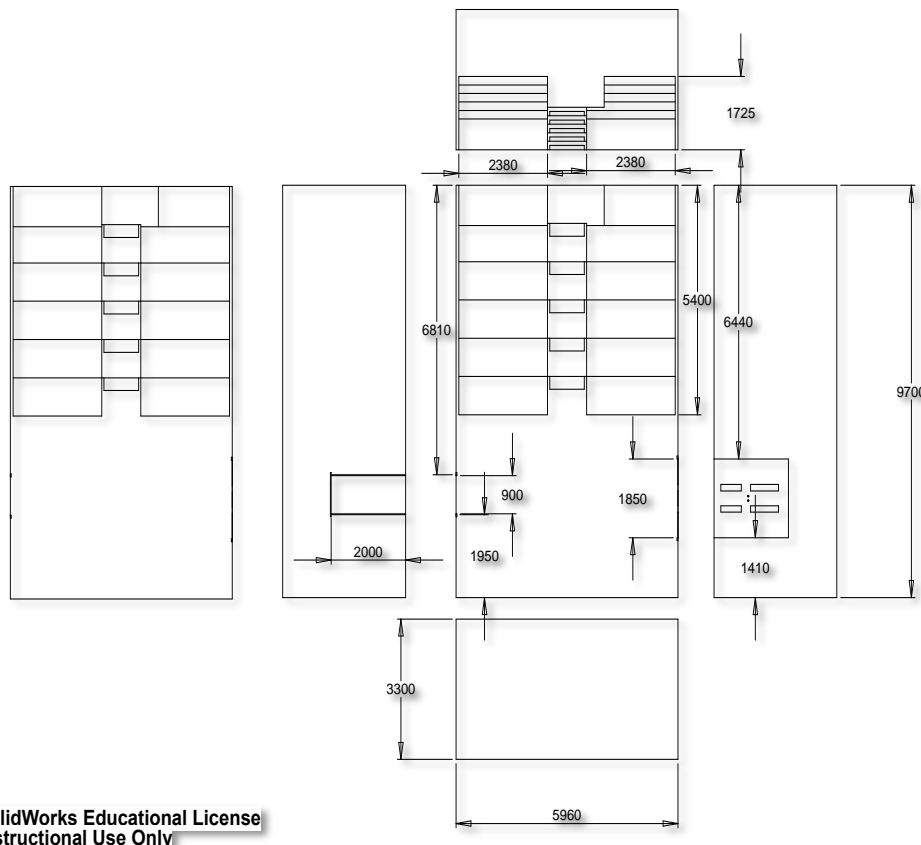


Figure 35 – Technical Drawing of Room 170 [32]

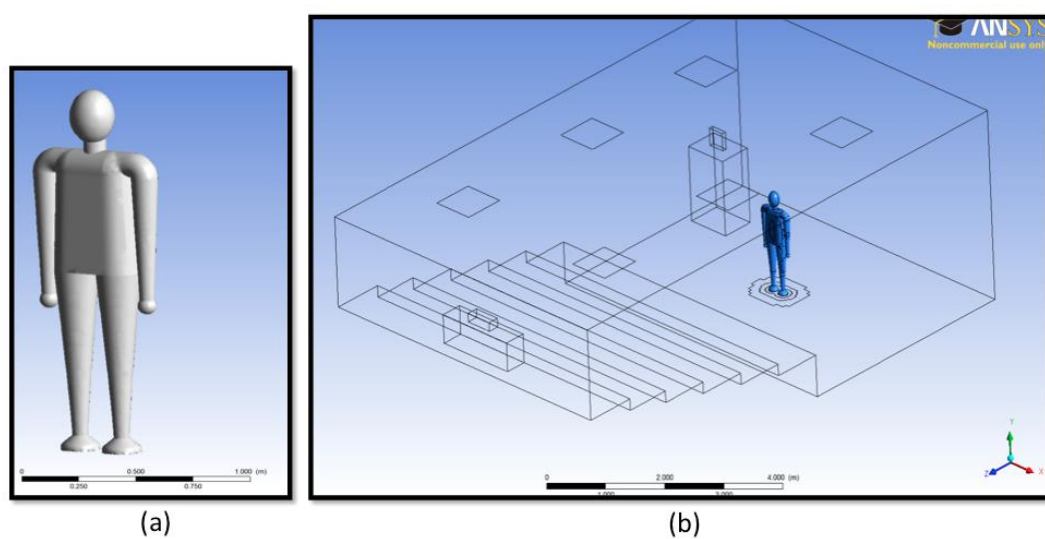


Figure 36 – Setup of Human Geometry in Room 170 [32]

Figure 37 shows the initial mesh used by Locci for simulations not containing the human. This was updated to contain the human geometry, seen in Figure 38. This is less refined than the mesh used for the natural convection due to the computational power available and the size of the domain. Despite this, the solution was successful with all residuals converging completely. All details relevant to the setup of the Room 170 case can be seen in Figure 39, whilst the method for obtaining ambient conditions for the Fiala model is displayed in Figure 40.

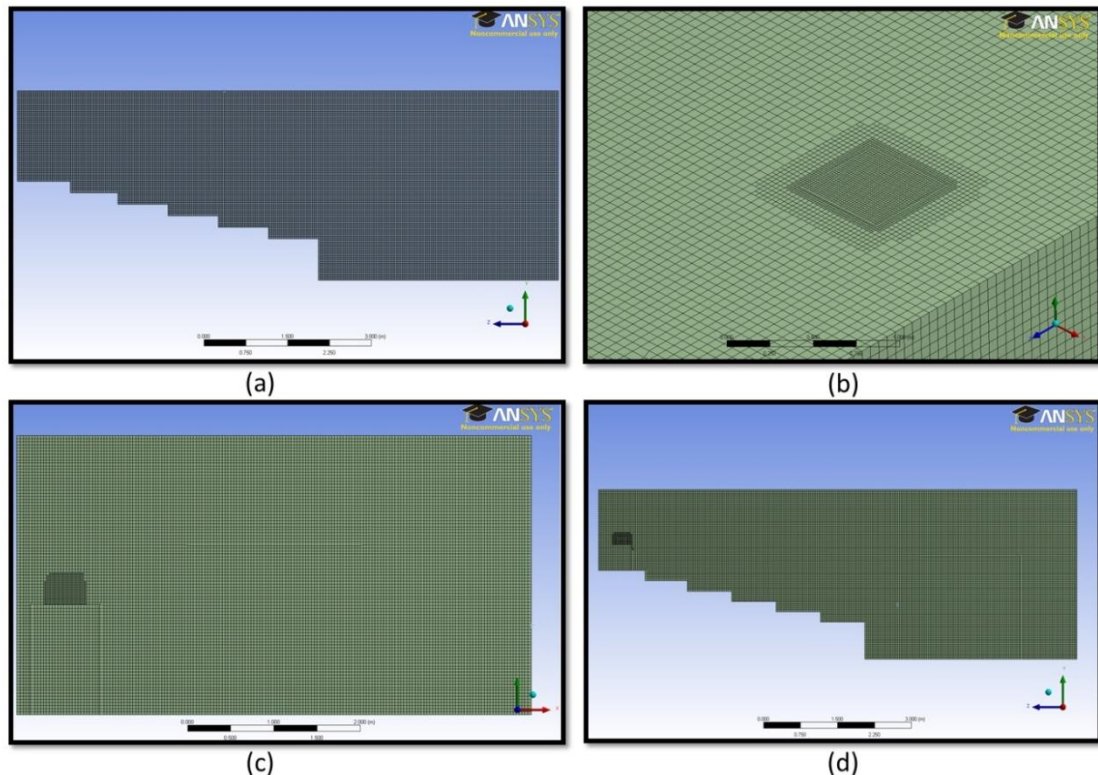


Figure 37 – Initial Mesh used by Locci

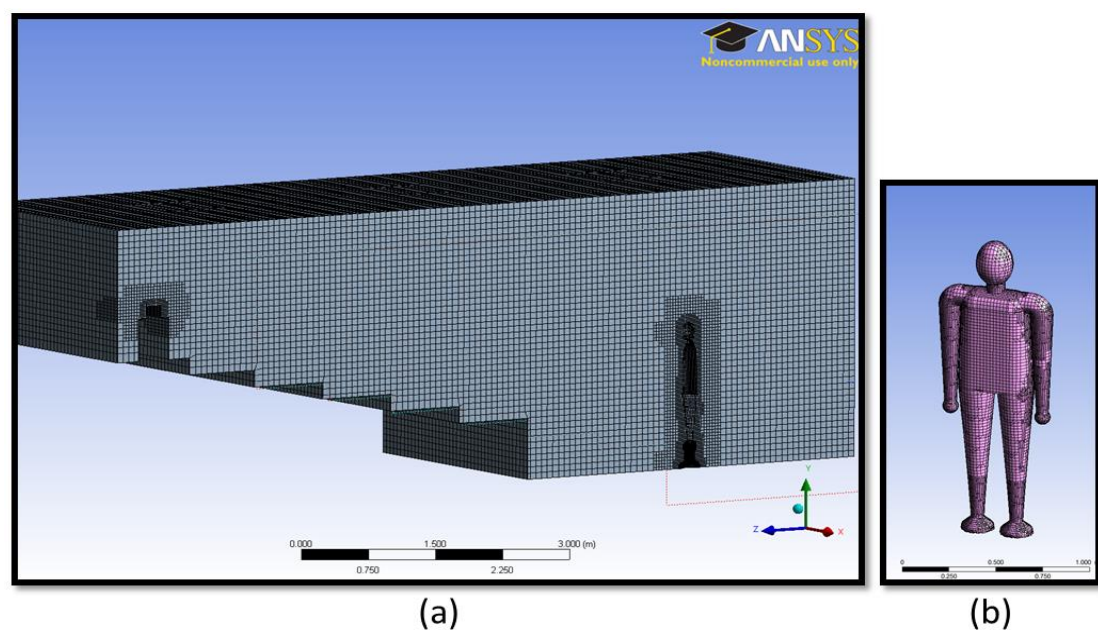


Figure 38 – Mesh of Room 170 Containing the Human Geometry

<u>Calculation Set-up</u>	<u>Fixed Boundary Conditions</u>
Type: Pressure-based	Constant Temperature Surfaces:
Time: Steady	• Lateral Walls: 293.1 K
Energy Eq.: On	• Back Wall: 293.4 K
Velocity: Absolute	• Front Wall: 293.2 K
Gravity: -9.81 m/s ²	• Floor: 291.2 K
Models: k-e Standard	• Ceiling: 294.4 K
Total buoyancy effects included	• Seats and Desks: 293.5 K
<u>Inlet 1,2,3 & 4:</u>	<u>Outlet:</u>
Type: Mass-flow Inlet	Type: Pressure Outlet
Direction: Vertically Down	(0 Pa)
Flow Rate: 1.0 Kg/s	
Gauge Pressure: 0.00 Pa	
Turbulence: Intensity 15% with	
Length Scale 0.5m	
Air Temperature: 291K	
<u>Computer</u>	<u>Fixed Boundary Conditions</u>
Type: Stationary Wall	Constant Temperature Surfaces:
- No slip conditions	• Projector Stand 293.5K
Constant heat flux: 238 W/m ²	• Computer Stand 293.1K
Heat generation rate: 8333W/m ³	
(60 Watts)	
<u>Projector</u>	Human Control Cube Volume:
Type: Stationary Wall	• Symmetry Conditions
- No slip conditions	to all 5 surfaces
Constant heat flux: 323 W/m ²	
Heat generation rate: 7111W/m ³	
(80 Watts)	

Figure 39 – Room 170 Setup Details

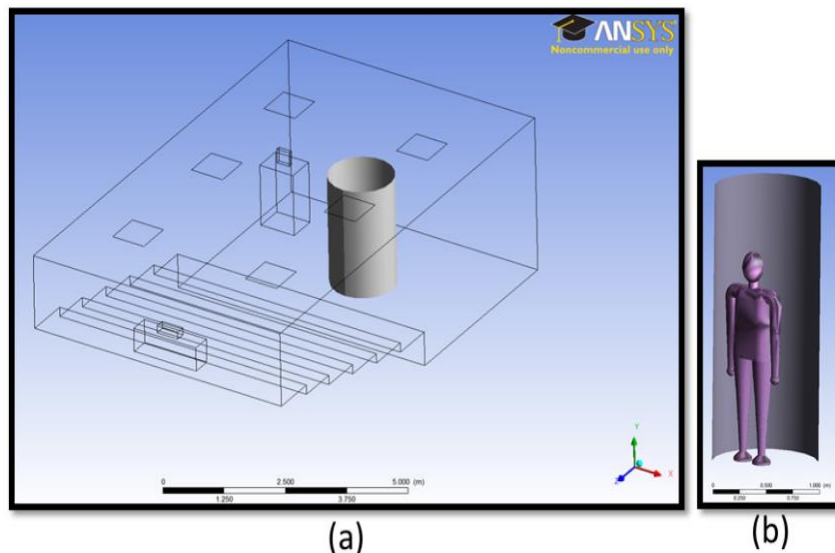


Figure 40 – Method Used for Obtaining Ambient Conditions for Fiala Input

Appendix E

As mentioned in the deliverables section, part of this project looked at obtaining thermal images. Due to the nature of thermal imaging obtaining temperature values from radiation, the results weren't entirely comparable to the CFD work. However they were still useful as they show a vast difference between temperature of clothing and skin, with the face and forehead clearly very hot. This is reflected in the outputs of the Fiala model when a clothing file was used. The pictures do not show air temperatures and therefore a thermal plume is not visible, as only surface temperatures are shown. Figure 41 shows two thermal images that were taken, one of Tompsett and one of myself, displaying the difference between skin and clothing temperatures, with the faces clearly the warmest area.

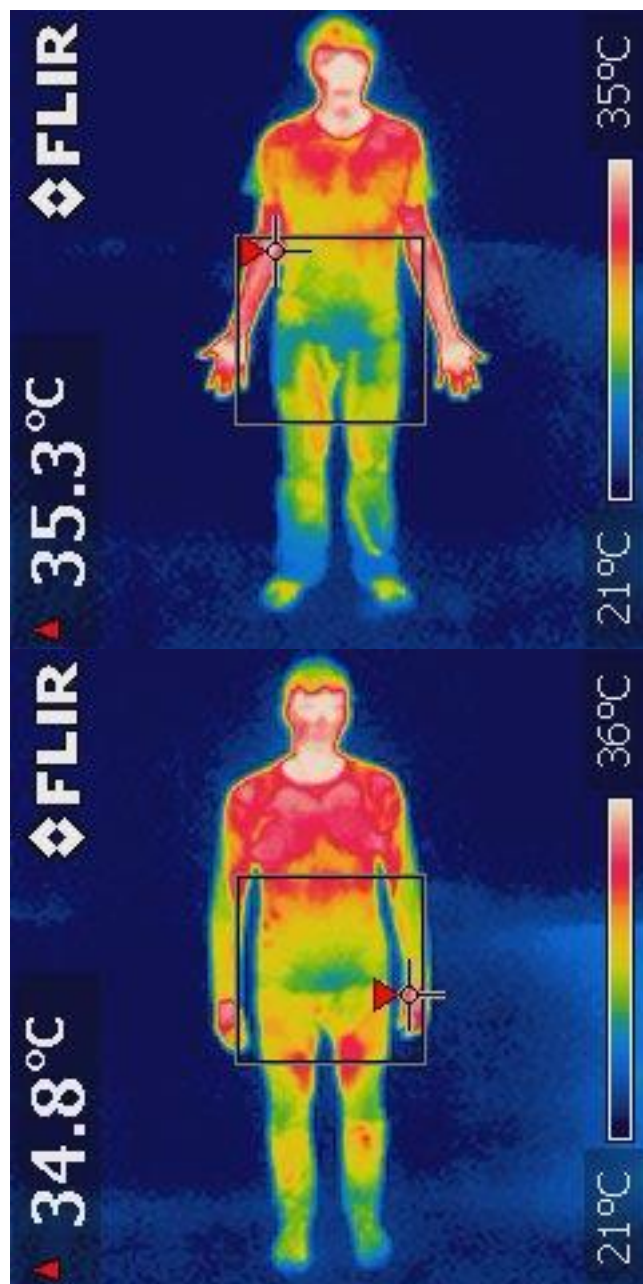


Figure 41 – Thermal Images of Tompsett (top) in t-shirt and trousers, and French (bottom) in jumper and trousers